Project Number: GTH-L101

QUADROTOR UAV INTERFACE AND LOCALIZATION DESIGN

A Major Qualifying Project
submitted to the Faculty
of the
WORCESTER POLYTECHNIC INSTITUTE
in partial fulfillment of the requirements for the
Degree of Bachelor of Science
by

_____

Brian Berard

_____

Christopher Petrie

_____

Nicholas Smith

Date: October 17, 2010

Approved:

_____

Professor George T. Heineman, Major Advisor

_____

Professor William Michalson, Major Advisor

Disclaimer: This work is sponsored by the Missile Defense Agency under Air Force Contract F19628-00-C-0002 (1Apr00-31Mar05). Opinions, interpretations, conclusions, and recommendations are those of the authors and are not necessarily endorsed by the United States Government.

ABSTRACT

MIT Lincoln Laboratory has expressed growing interest in projects involving Unmanned Aerial Vehicles (UAVs). Recently, they purchased a Cyber Technology CyberQuad quadrotor UAV. Our project's task was to assist the Laboratory in preparation for the future automation of this system. In particular, this required the creation system allowing computerized-control of the UAV – specifically interfacing with the software tools Lincoln Laboratory's Group 76 intended use for future development, as well as a high-accuracy localization system to aid with take-off and landing in anticipated mission environments.

We successfully created a computer control interface between the CyberQuad and Willow Garage's Robot Operating System used at the Laboratory. This interface could send commands to and receive responses from the quadrotor. We tested the performance of the quadrotor using our interface and compared it against the original analog control joystick. Latency and link health tools were developed, and they indicated that our solution, while clearly less responsive than the analog controller, would be usable after minor improvements.

To enable localization we investigated machine vision and video processing libraries, altering the augmented reality library ARToolKit to work with ROS. We performed accuracy, range, update rate, lighting, and tag occlusion tests on our modified code to determine its viability in real-world conditions. Ultimately, we concluded that our current system would not be a feasible alternative to current techniques due to inconsistencies in tag-detection, though the high accuracy and update rate convinced us that this localization method merits future investigation as new software packages become available.

TABLE OF CONTENTS

TABLE OF FIGURES

TABLE OF TABLES

EXECUTIVE SUMMARY

Recent technological advances in robotics and aeronautics have fostered the development of a safer, more cost-effective solution to aerial reconnaissance and warfare: the unmanned aerial vehicle (UAV). These devices provide many of the same capabilities as their manned counterparts, with the obvious advantage of reduced human risk. Already, many of surveillance missions traditionally requiring a trained pilot and multi-million dollar piece of equipment can be performed by less-trained individuals using cheaper, smaller UAVs.

Following the trend of military interest in UAVs, MIT Lincoln Laboratory has expressed a growing interest in UAV projects. More recently, they purchased a Cyber Technology CyberQuad quadrotor UAV. It was our project's goal to assist the Laboratory in preparation for the future development of this system. In particular, we required: 1) a means by which to communicate with the UAV directly using a computer running Lincoln Laboratory Group 76's current software development platform, and 2) a localization system that could be used to assist automated quadrotor take-off and landing in anticipated mission environments.

METHODOLOGY

Creating an interface between the CyberQuad and Willow Garage's Robotic Operating System (ROS) required implementing a system which utilized CyberQuad's existing serial protocol. The CyberQuad product is based on the open-source compilation of hardware and software made by the German company MikroKopter, which is specifically designed for UAV development. The MikroKopter system includes the ability to connect to communicate with a PC via a wired serial link for the purpose of limited debugging. Achieving full computer control of the CyberQuad, however, required handling of additional quadrotor messages – control functionality not present in the commercial software, yet made available in MikroKopter firmware. Additionally, this functionality was encapsulated within the fundamental structure of ROS, a *node*, to ensure compatibility with the other robotic platforms in use at the Laboratory.

To address the issue of localization, we chose to investigate the field of machine vision. Rather than attempting to write the vision processing code ourselves, we utilized an augmented reality (AR) software library. This library included functionality to determine the location and orientation of specific high-contrast, pattern-based tags in respect to a camera. We encapsulated the functionality of the library we chose (ARToolKit) into a form compatible with ROS and designed a simple program to pass the library's output data into native ROS structures that could be accessed by other ROS processes.

RESULTS

The localization scheme we developed was tested for accuracy and robustness to determine its viability in real-world quadrotor applications. Using a webcam as an analog to the CyberQuad's on-board camera, we ran accuracy, range, update rate, variable lighting, and tag occlusion tests with our modified library. The system performed within our specified accuracy and update rate requirements. Additionally, the detection range of the software was a function of tag scale, suggesting that the range requirements specified by our design specifications (0.5-15 ft) would be obtainable. Our testing, however, revealed a number of issues that might prevent immediate real-world system application. Variable lighting and minimal tag obstruction both proved to be of major concern in reliable tag recognition.

We demonstrated the functionality of our CyberQuad-PC interface system with a ROS gamepad, frequently used by Group 76, to demonstrate proper communication between ROS and the CyberQuad. We also tested the tools that we designed to monitor the wireless link between computer and CyberQuad. Using this link monitor, we were able to calculate average message latency and the amount of messages dropped by the wireless serial link that we employed.

Finally, we demonstrated the integration of the systems by creating a control loop to move the UAV to a set location in space using only our localization code as feedback. Using ROS transform-visualization tools, we were able to determine that the correct error between the

desired position and UAV's current location was generated correctly. From debugging messages, we were also able to conclude that the correct commands were being sent to the quadrotor to correct for this error. However, the physical responses of the CyberQuad never truly matched the anticipated motions. We suspect this is a result of compound latency issues that were exhibited by both the localization and interface systems. The irregular performance of the localization system and limited control rate of the interface also likely contributed to the erratic behavior.

CONCLUSION

Our experiences with the localization system and quadrotor interface led to the conclusion that extensive work is required before either system is ready for real-world application. This project demonstrated that computer vision-based localization is a tool worth further investigation, mainly due to its ability to function in GPS denied locations. The current system that we provided to Lincoln Laboratory will never function reliably in real-world conditions, based on the shortcomings of the vision system in the areas of light compensation and tag obstruction. Future work should focus on replacing the outdated computer vision processing algorithms used in this project with more modern commercial libraries. Additionally, research should continue into sensor fusion between vision-based localization data and the CyberQuad's on-board sensor data.

Although the interface we developed for the CyberQuad functions as our design specifications required, the data-rate limitations and latency in the wireless serial link make research into alternative approaches to quadrotor UAV communication schemes necessary. In the current iteration, a significant portion of the computer's resources were required to communicate with the UAV. We suspect that much more effective methods of achieving UAV automation can be implemented by creating a computer-controlled analog control emulator (essentially a serial controlled version of the existing CyberQuad analog controller) or by

offloading high-precision trajectory calculations and localization into the CyberQuad's firmware to avoid serial data-rate limitations.

1.0 INTRODUCTION

Current high-tech, complex military operations require a high degree of real-time target and mission-relevant information. The US military frequently depends on airborne reconnaissance to deliver this information. In the past, manned aircraft with onboard cameras and other sensors have had a primary role in airborne intelligence operations. More recently, however, technological advances have allowed unmanned aerial vehicles (UAVs) to carry out reconnaissance missions in the place of the conventional manned aircraft. For the purpose of this report, we use the Department of Defense (DoD) definition of UAVs: "powered aerial vehicles sustained in flight by aerodynamic lift over most of their flight path and guided without an onboard crew" [1].

Systems deployed today are generally significantly smaller than manned aircraft, yet larger than a traditional model airplane. They generally carry a highly sophisticated payload of sensors and surveillance cameras and are designed to be operated semi-autonomously using a remote operation-based control scheme [1].

MIT Lincoln Laboratory recently began investigating a new class of UAVs with different mission capabilities and intended applications. In particular, researchers have started work with "quadrotor" rotorcraft systems to explore potential future applications. Quadrotors are non-fixed-wing rotorcraft platforms that utilize four propellers to achieve vertical lift and maneuver through the air. Our project supported this exploratory effort by investigating the newly available CyberQuad Mini quadrotor platform, (developed by Cyber Technology) by designing a software codebase for future quadrotor projects at MIT Lincoln Laboratory.

Although quadrotor systems are new to Lincoln Laboratory, a number of the Lab's recent robotics applications – in areas other than UAVs– use a standardized robotic development framework, known as ROS (Robotic Operating System), to streamline the process of development. The newly-acquired CyberQuad system, however, does not integrate with ROS - a problem for engineers looking to preserve a laboratory-wide standard. To enable a consistent

development platform, we first needed to integrate the UAV's built-in software, produced by the German company *MikroKopter*, with ROS. An interface between the two was the necessary first step toward providing Lincoln Laboratory with a foundation for further investigation of quadrotor UAVs.

Additionally, our team sought to perpetuate MIT Lincoln Laboratory's knowledge of collaborative aerial and ground based robotic systems. Quadrotor UAVs have a number of potential applications when integrated with existing unmanned ground vehicles (UGVs), including joint terrain mapping, reconnaissance, target tracking, and more. These applications, however, often exceed the maximum operating time allowed by the quadrotor's onboard batteries. During the mission, the quadrotor will undoubtedly require recharging or possibly repairs. Therefore, before truly autonomous aerial-ground collaborative robotic missions could be feasible, the UAV must be capable of locating its ground-based counterpart and executing a landing. The first step toward a precise, safe landing, however, lies in locating the ground-based system and calculating the UAV's relative position to the landing platform. As such, we sought to create a robust localization system for the UAV that was both practical and precise in real-world environments at ranges at which GPS navigation is impractical.

A number of past quadrotor projects performed at other institutions have employed advanced object-tracking systems that are unsuitable in terms of this particular task. Many of these systems employ rooms comprised of position-finding cameras, high-resolution GPS modules, or other expensive equipment to determine the quadrotor's position. On the other hand, some of the existing work in this field has involved cheap, consumer devices to provide a solution. Our goal was to create a quadrotor control system that is suitable for real-world scenarios involving only the CyberQuad UAV and collaborating ground-based vehicle.

.

In particular, we employed the CyberQuad Mini quadrotor UAV, provided by MIT Lincoln Laboratory, as the primary focus of our development. This rotorcraft system is outfitted with a camera, which allowed for the vision-based localization element that was one of the foci of this project. We used the open-source robot operating system (ROS) provided by Willow Garage to interface with the CyberQuad hardware and software. Due to the limited time constraints, we simulated the ground-based vehicle with a Linux-based computer and a mock-up landing platform for testing.

We established three major goals to guide us toward the successful realization of our overarching goal for UAV-UGV collaboration:

- Develop a PC control interface for the CyberQuad system
- Enable precise UAV localization
- Provide documentation to enable continued development of the CyberQuad system

These goals led to the development of an end product that could be utilized by future MIT Lincoln Laboratory researchers. Additionally, to showcase our efforts, our team developed a number of demonstration materials that both encapsulate the work that we accomplished and that help illustrate the abilities and potential applications of the system.

This paper discusses the process by which these steps were completed, major design decisions, and the results achieved. We also provide a set of recommendations for continued work with the quadrotor UAV by MIT Lincoln Laboratory.

1.1 METRICS FOR SUCCESS

At the beginning of the project, we developed the following metrics to evaluate the success of this project. These metrics were applied throughout the project to ensure that the project's

outcomes were consistently guided. This section should act as a rubric against which the project should be measured. These metrics are:

1. The project should produce a wireless communications scheme that allows sensor and control information to be transmitted easily between the UAV and a ROS-enabled computer. The system should be extendable to support communication between multiple UAV systems, as well as be generic enough to port easily to other UAV platforms.
    a. The API created for the UAV must provide users with a convenient means of communication with the quadrotor, but must also provide complete visibility for the benefit of future developers. For the purposes of logging, playback, and visibility, all commands must be sent in the form of ROS topic messages.
2. A simple control loop should be produced, having wireless control over the motion of the UAV in real time. Minimally, open-loop vertical, directional, and rotational controls need to be supported. Optimally, this would also allow for low-level control adjustments. The system must be able to continue sensor feedback communication during control procedures as well.
    a. A test fixture is required to demonstrate functionality in the computer control of the UAV. This fixture must hold the quadrotor in place so that no damage will be sustained, but also must allow for enough movement to demonstrate that external control is functional.
3. The PC controller must be able to wirelessly query the state of the UAV sensors in real time. In our system, the state of each onboard sensor should be received at a user-specified interval.
4. The project should produce a system which allows UAV location and orientation information to be determined visually in an indoor environment by means of computer

vision. The localization scheme employed should have the capacity to function in an outdoor environment as well, though outdoor testing may be impractical.

   a. This vision system must be viable for real-world, outdoor environments. As such, it must take into account conditions which make visual systems inoperable or cause problems. Thus, the final project should be able to be moved out of a closed testing environment and still be able to function under normal weather conditions.

5. The computer vision should be able to produce position information which is measurably more precise and accurate than GPS and other available systems in close-range scenarios. While the position and orientation of the UAV should be able to be determined within the specified range of 0-15 feet, we must demonstrate increased precision when within 0-5 feet of the UGV platform.

   a. The localization method chosen must provide position knowledge at a range of 15 feet with a 12-inch tracking target, or “tag”. It also must provide tag detection at a minimum range of 6 inches. At all ranges, the localization system must have an average error of less than 50 centimeters.

2.0 BACKGROUND

The safe take-off, operation, and landing of UAVs traditionally require a pilot with extensive training [2]. These pilots must be trained to carefully handle these large, expensive vehicles and execute difficult landing and take-off maneuvers similar to those of a manned fighter. More recently, however, work has been done to automate these complex procedures [3]. These developments reduce the possibility of human error, and reduce the amount of training required to operate the craft.

The emerging quadrotor UAV technologies offer a solution to the complications inherent in the operation of traditional UAVs. These systems offer a simpler solution that will allow even untrained pilots to operate the quadrotor. With the growing interest in quadrotors, however, a higher level of development and functional maturity is required for successful deployments of the new technology. While quadrotors are capable of more complex maneuvers than fixed-wing aircraft, granting a higher potential for more complex autonomous behaviors, the technology has not yet advanced to the point that they can be employed in real-world situations. Their potential for a more advanced mission repertoire makes research into their operation key for the advancement of autonomous, or simply computer-augmented control.

At present, fixed-wing UAVs employ complex navigational systems comprised of high-accuracy global positioning systems (GPS) and internal instrumentation. Their inertial guidance systems (IGS) contain compasses, accelerometers, and gyroscopes to provide relative position information to the UAV. While the GPS and IGS-based navigation schemes are practical for most fixed-wing UAVs deployed today, these navigation methods may prove inadequate in future quadrotor applications.

Several shortcomings in current localization techniques exist for quadrotor UAVs [4]:

- Traditional systems are often bulky; they do not fit rotorcraft payload limitations.
- Traditional systems do not provide object-to-object relative orientation information.

- Traditional systems (i.e. GPS) do not provide accurate elevation information.
- GPS requires a clear view of the sky and is not available in some deployment situations.

As UAVs become increasingly complex, the control mechanisms must also become more sophisticated. Therefore, an increased level of automation is required to use these systems them to their full potential. To enable automated control, UAVs must provide detailed information about their position and orientation in their environment. Given the complex maneuvers possible with rotorcraft, this information must be very detailed including positions relative to targets and obstacles. Other positioning system often do not provide this object-to-object relative data, instead relying on a global frame of reference (GPS), or self-relative (IGS) with compounded error. Because the technologies in deployment today are not suitable for quadrotor aircraft to accomplish these goals, a new localization method must be employed.

2.1 THE QUADROTOR

The first step toward completing our project was to research the CyberQuad Mini system with which we would be working over the course of the project. This quadrotor used in this project will be MIT Lincoln Laboratory's UAV application development platform in the future, and an understanding of its operation and construction is important both to this as well as any future projects. This section provides specific details of the specifications of this particular UAV.

2.1.1 SPECIFICATIONS

The hardware system employed in this project is a quadrocopter rotorcraft (or "quadrotor") UAV manufactured by Cyber Technology in Australia, called the CyberQuad Mini. This Vertical Take-Off and Landing (VTOL) aircraft focuses on simplicity, stability, safety, and stealth [5]. The number of available features and payload options allow for a wide range of potential applications.

FIGURE 1: THE CYBERQUAD MINI

The CyberQuad Mini features four ducted fans, powered by brushless electric motors, for safety and durability. Its small form factor allows for a wide range of short-range operating conditions, particularly in the urban environment. The CyberQuad Mini's more specific physical technical specifications are as follows:

TABLE 1: CYBERQUAD TECHNICAL SPECIFICATIONS

Dimensions	420mm x 420mm x 150mm (~16.5in x ~16.5in x ~5.9in)
Airspeed	50 km/h (~31mph)
Payload	500g (~1.1lbs)
Endurance	~25min of flight
Altitude	1km (video link)
Range	1km (video link)
Noise	65dBA @ 3 m

The CyberQuad Mini possesses varying levels of autonomy. While the UAV can be controlled by a wireless handheld controller, some flight functions are controlled by the on-board hardware; the robot has built-in control for attitude and altitude and features optional upgrades for heading hold and waypoint navigation. The attitude and altitude control keeps the CyberQuad level and limits tilt angles to prevent the pilot from overturning the UAV during flight; this control also maintains altitude while limiting the maximum height and rate of climb and decent [5]. The next level of autonomy involves the on-board GPS and 3D magnetometer to enable the quadrotor to maintain its position, compensating for wind drift. These sensors can also be used to remember the robot's "home" position and to return to it autonomously. The final implemented level of autonomy utilizes GPS waypoint navigation to control the UAV via a pre-programmed route with auto take-off and landing.

This UAV system also contains a number of Cyber Technology's optional quadrotor features in addition to the basic setup - one of which being the real-time video camera. With VGA video resolution of 640x480, a low-light CCD sensor, replaceable lenses for varying field of view, gyro-stabilized and servo-controlled elevation, and a 5.8GHz analog video transmitter, the CyberQuad is able to supply video to an off-board system allowing the operator to fly the UAV in real time even without direct line of sight to the rotorcraft.

Another feature is the handheld controller for manual manipulation, experimentation, and testing. It sports two analog control sticks (one controlling thrust and yaw and the second control pitch and roll) and a number of buttons for controlling previously described features while the system is in flight. Additionally it has a LCD display that allows the monitoring of many of the CyberQuad's internal sensors. This 12-channel transmitter with a 5.8GHz video receiver, coupled with the included video goggles, allows the operator to control the UAV with precision from a distance of roughly 1km (according to the specifications).

The final addition to the CyberQuad present in Lincoln Laboratory's model is the navigation upgrade. In order to operate in "full autonomous" mode, the robot required GPS and

3D magnetometer information. This upgrade provided the required sensors to allow for built-in autonomous heading hold and waypoint navigation.

2.2 MIKROKOPTER

The CyberQuad Mini electronics are provided by the German company *MikroKopter*, which is an open-source solution for quadrotor control. This hardware and software solution contains necessary functions for controlled flight, as well as additional functionality for retrieving data from on-board sensors.

2.2.1 MIKROKOPTER HARDWARE

The MikroKopter control hardware in the CyberQuad platform is divided into several core modules that control different aspects of the device: FlightCtrl, BrushlessCtrl, NaviCtrl, MK3Mag, and MKGPS. Each module adds different functionality or sensors to the quadrotor. All of the modules above were present in this project's UAV. Additionally, a pair of 2.4 GHz ZigBee XBEE Bluetooth transceivers is used to establish the serial link between the MikroKopter and the ROS enabled computer.

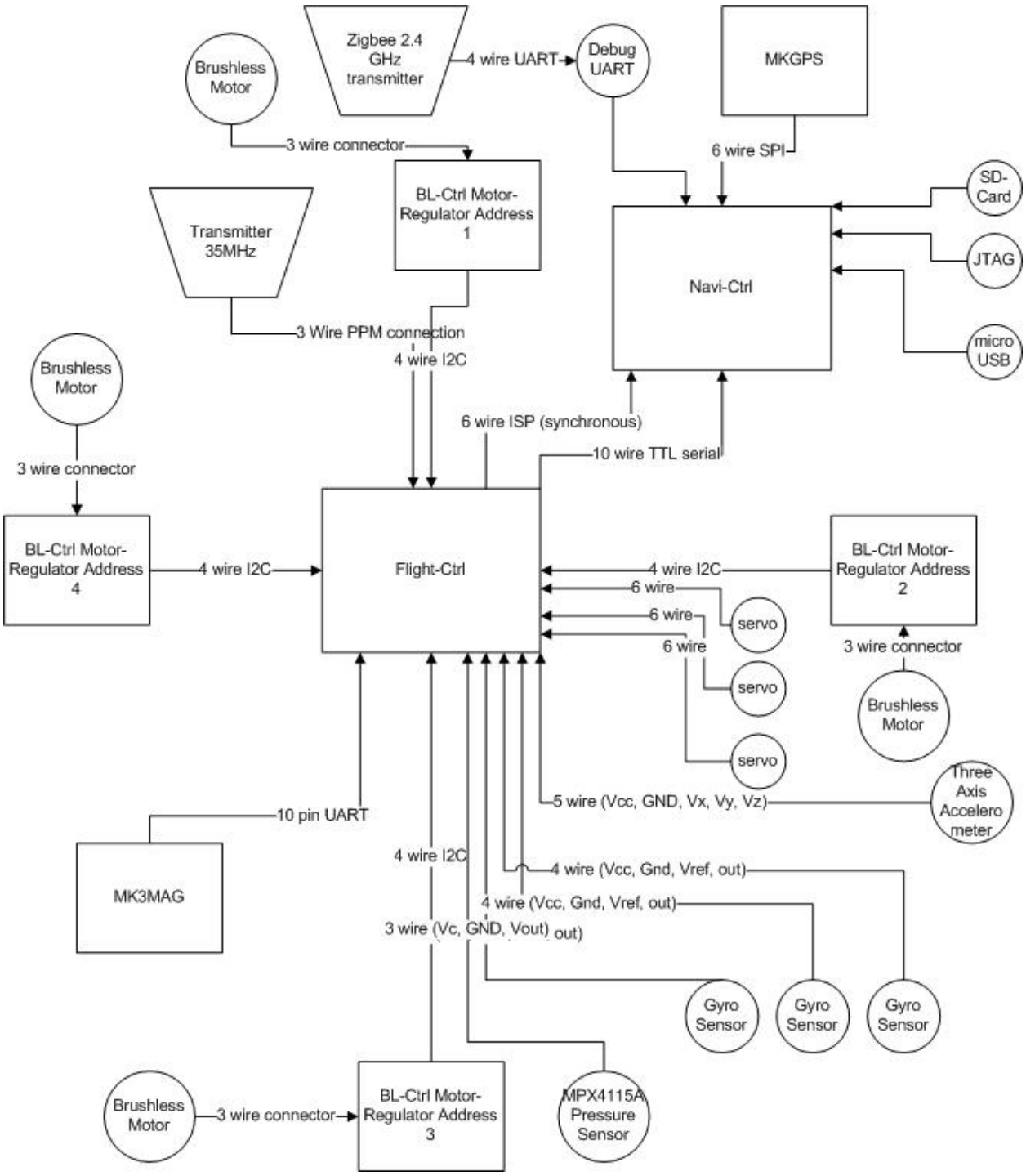

FIGURE 2: MIKROKOPTER HARDWARE ARCHITECTURE

FLIGHTCTRL

FlightCtrl manages flight-related functions of the MikroKopter device. This module is controlled by an Atmega 644p microprocessor, which manages several onboard sensors necessary to maintain stable flight. Three gyroscopes are used to determine the rate of angular rotation about the X, Y, and Z axes, allowing FlightCtrl to maintain the aircraft's directional orientation. Additionally, a three-axis (X, Y, Z axes) accelerometer is used to maintain level flight. Lastly, an onboard barometric sensor allows approximate altitude to be maintained, when the system is sufficiently elevated during flight.

FlightCtrl supports two methods of communication to and from the device. It handles the input from a radio receiver, allowing the MikroKopter to be controlled remotely from a traditional analog wireless controller. It also supports communication over an I2C bus, allowing the board to relay sensor and motor-control data and to receive flight control parameters from other MikroKopter modules.

BRUSHLESSCTRL

BrushlessCtrl controls the speed of the four brushless flight motors. While this module can be controlled using various interfaces (I2C, serial, or PWM), it is controlled by FlightCtrl by default via I2C.

NAVICTRL

NaviCtrl allows for remote computer control and communication over a serial link. This module has an ARM-9 microcontroller at its core, managing the connection to the MKGPS (GPS) and MK3Mag (compass) modules, handling request/response user commands via the serial link, and sending movement commands back to FlightCtrl. By communicating with the GPS and compass modules, this device allows the MikroKopter to hold its position and orientation with respect to the global (world) coordinates, as well as to navigate to different coordinates using waypoints.

MK3MAG

MK3Mag and MKGPS interface directly with the NaviCtrl module through header connections. MK3Mag is a magnetometer (compass) module providing orientation data with respect to magnetic north. This sensitive sensor must be calibrated before each flight, and must remain some distance from intense EMF-emitting devices to ensure accuracy. MKGPS is a Global Positioning System (GPS) module providing absolute global coordinates. This sensor requires no calibration, but must have a clear view of the sky to function properly.

WIRELESS COMMUNICATION

The ZigBee XBEE-PRO Bluetooth adapter pair allows for a wireless communications between the PC and MikroKopter hardware via a 2.4GHz network-protocol serial link. Specifically, the XBEE that was added to the CyberQuad was connected to the NaviCtrl module via its serial debug port. This serial interface allows for access to useful FlightCtrl, NaviCtrl, and MK3Mag control mechanisms, and provides all interfaces to remotely control the CyberQuad and receive sensor feedback.

2.2.2 MIKROKOPTER SOFTWARE

All communication with MikroKopter hardware will take place over the serial interface provided by NaviCtrl. This module implements the MikroKopter serial interface format and enables for 2-way communication (PC to device) with all onboard modules, using command and response messages of varying lengths.

TABLE 2: MIKROKOPTER SERIAL PROTOCOL

Start Byte	Device Address	Command ID	Data Payload	Checksum	End Byte
#	1 Byte	1 Byte	Variable length message	2 Bytes	\r

Specifically, all messages are in the following format: Start Byte (always "#"), Device Address Byte (1 for FlightCtrl, 2 for NaviCtrl, 3 for MK3Mag), Command ID Byte (a character), N Data Bytes (any number of bytes, including zero), and two Bytes for Cyclic Redundancy Check (CRC), and finally the Stop Byte (always a "\r"). Each PC command may or may not produce a resulting response from the MikroKopter software; however, if a response is sent, the Command ID Byte character returned is the same character as was sent by the PC, but with the character case inverted (upper case characters become the equivalent lower case letters and vice versa).

There are approximately 30 distinct serial commands that can be sent to the MikroKopter, producing about 23 different responses. A list of these commands and their responses taken directly from the MikroKopter website [6] can be found below in

Table 3: Common Commands, Table 4: FlightCtrl Commands, and Table 5: NaviCtrl Commands. Some responses are simply a "confirm frame" signifying the command was successfully received, while others return information about the state of the MikroKopter. Specifically, the commands are broken down into four classifications: Common, FlightCtrl, NaviCtrl, and MK3Mag commands. Common commands return high level system information (such as the data text to hand-held controller's display), as well as providing the means for remote movement control (with a similar abstraction as the hand-held controller). FlightCtrl commands provide the means for reading and writing low level system parameters, as well as a means of testing the motors. NaviCtrl commands provide a means for sending waypoints and receiving sensor data, as well as testing the serial port. MK3Mag command provides attitude information, though are only used internally.

TABLE 3: COMMON COMMANDS

Command	Data from PC	Data from MK
Analog Values	u8 Channel Index	u8 Index, char[16] text
ExternControl	ExternControl Struct	ConfirmFrame
Request Display	u8 Key, u8 SendingInterval	char[80] DisplayText
Request Display	u8 MenuItem	u8 MenuItem, u8MaxMenu, char[80] DisplayText
Version Request	-- blank --	VersionInfo Struct
Debug Request	u8 AutoSendInterval	Debug Struct
Reset	-- blank --	N/A
Get Extern Control	-- blank --	ExternControl Struct

TABLE 4: FLIGHTCTRL COMMANDS

Command	Data from PC	Data from MK
Compass Heading	s16 CompassValue	Nick, Roll, Attitude...
Engine Test	u8[16] EngineValues	N/A
Settings Request	u8 SettingsIndex	u8 SettingsIndex, u8 Version, u8 Settings Struct
Write Settings	u8 SettingsIndex, u8 Version, Settings Struct	u8 Settings Index
Read PPM Channels	-- blank --	s16 PPM-Array[11]
Set 3D-Data Interval	u8 Interval	3DData Struct
Mixer Request	-- blank --	u8 MixerRevision, u8 Name[12], u8 Table[16][4]
Mixer Write	u8 MixerRevision, u8 Name[12]	u8 ack

Change Setting	u8 Setting Number	u8 Number
Serial Poti	s8 Poti[12]	-
BL Parameter Request	u8 BL_Addr	u8 Status1, u8 Status2, u8 BL_Addr, BLConfig Struct
BL Parameter Write	u8 BL_Addr, BLConfig Struct	u8 Status1, u8 Status2

TABLE 5: NAVICTRL COMMANDS

Command	**Data from PC**	**Data from MK**
Serial Link Test	u16 EchoPattern	u16 EchoPattern
Error Text Request	-- blank --	char[] Error Message
Send Target Position	WayPoint Struct	-
Send Waypoint	WayPoint Struct	u8 Number of Waypoints
Request Waypoint	u8 Index	u8 NumWaypoints, u8 Index, WayPointStruct
Request OSD-Data	u8 Interval	NaviData Struct
Redirect UART	u8 Param	-
Set 3D-Data Interval	u8 Interval	3DData Struct
Set/Get NC-Param	?	-

Software written by and for the MikroKopter development team is a primary resource for developing the software interface. The exact format of the structures sent over the serial link can be found in the NaviData project code available online, and examples of usage can be found in the QMK Groundstation project code. The QMK Groundstation project [7] is similar to the goal of this project, as it provides a limited interface to the MikroKopter hardware (albeit a graphical interface) from a desktop computer. As such, it has some similar input/output functionality implemented, and was a springboard for development.

2.3 ROS

Willow Garage' Robotic Operating System (ROS) is an open-source project, specifically aimed at the integration of robotic systems and subsystems [8]. Designed to operate either on a single computer or over a network, ROS provides an inter-system communication framework, allowing for message passing both locally and over a network, as shown in Figure 3. This "meta-operating system" provides a number of services to simplify the development of advanced robotic systems. Namely, it provides:

- Hardware abstraction
- Low-level device control
- Implementation of commonly-used functionality
- Message-passing between processes
- Package management

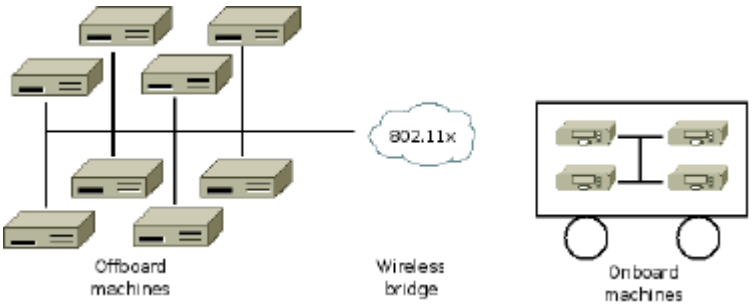

FIGURE 3: A TYPICAL ROS NETWORK CONFIGURATION

ROS was developed to be highly extendible, currently having integration with client libraries of C++ and Python (with more to come).The client libraries provide the interfaces with the ROS communication framework, as well as other advanced features. Using this system, executables written in different languages, perhaps running on different computers, can easily communicate if necessary. . In this project, however, we will be strictly using C++ for development.

ROS is designed to operate across multiple computers, providing a convenient method for writing and running code between systems and users. All code in ROS core libraries and applications is organized into *packages* or *stacks*. Packages are the lowest level of ROS software organization, containing code, libraries, and executables. These packages may contain any amount of functionality. The idea, however, is to create a new package for each application. For example, in Figure 4, a package would exist for each the camera, the wheel controller, and the decision-maker of a robot. Stacks are collections of packages that form a ROS library or a larger ROS system.

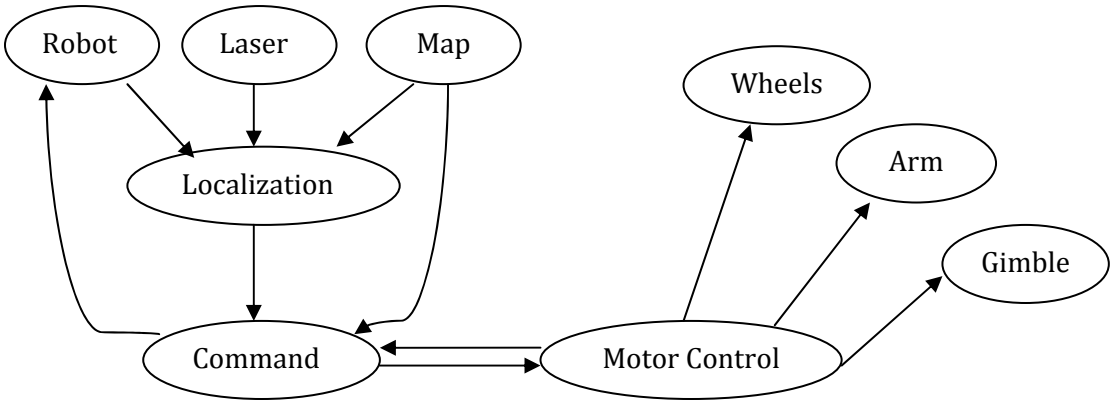

FIGURE 4: AN EXAMPLE ROS SYSTEM

The actual operation of ROS is based on executables called *nodes*. Ideally, each ROS package contains no more than one node. These nodes each operate as a separate application and utilize the ROS message scheme to communicate. In the example in Figure 4, above, the user would have created a ROS stack (My_Stack). In this stack, there exist nine different packages, one for each of the above nodes. Each package contains its own message definitions, source code, header files, and executable. The diagram depicts the directions of communication between the nodes. The “Command” node controls the entire system, receiving data from all of

the various navigation and control systems. It then sends commands to the robot and to the motor controller to direct the robot's actions.

In ROS, these nodes have two primary methods of communication between one another: asynchronous topic-posting and synchronous request/response. The method preferred at MIT Lincoln Laboratory employs asynchronous data transfer using various, user-defined "topics". ROS, however, also provides a request/response, synchronous communication scheme known as "services". ROS also allows parameters from nodes anywhere in the system to be stored in a global parameter server.

In ROS, data is transferred between nodes in the form of *msgs* (messages). *Msg* files are simple text files that describe the format and data fields of a ROS message. These messages can contain primitive data types (signed or unsigned int8, int16, int32, int64), floats (float32, float64), strings, times, other msg files, and arrays of variable or fixed length.

ROS's asynchronous style of data transfer utilizes *msgs* continuously posted to *topics* from which other nodes may read. A node will "publish" to a topic at pre-defined intervals, independent of other ROS operations. Any number of nodes may "subscribe" to this topic. The subscribers, however, need not be at the same level in the ROS hierarchy to subscribe to a topic - topics are globally visible. When a node subscribes to a topic, it will constantly listen for a posting to that topic, and when received, will execute a certain command.

The other form of ROS communication is the synchronous scheme, executed by *services*. A *srv* message is comprised of two parts: a request and a response. A node that provides a service operates normally until it receives a request for one or more of its services. This "request" will contain all of the parameters defined in the *srv* message. The node will then execute its service function and return the "response" defined in the *srv* message.

Each system of communication comes with advantages and disadvantages. The primary advantage of topics is visibility. Any node in the entire system may access a topic and see the data. Additionally, topics can be logged into a *.bag* file for later analysis, and may even be used

to replay events. These topics, however, only transmit data in one direction. Bi-directional communication between two nodes requires two topics, between three nodes requires three topics, and so on. On the other hand, services are perfect for bi-directional communication on a "need-to-know" basis. Any node in the system may access a node's service, give it data, and receive the data needed in return. Services, however, are not as easily logged and cannot be replayed later using bag files.

2.4 LOCALIZATION:

Many practical applications of UAVs require that the craft determine its position in space relative to some coordinate frame while in motion. These reference frames can be internal (IGS), global (GPS), relative to a pre-defined coordinate system, or relative to an external object. The UAV's ability to localize itself in these reference frames is entirely dependent on the method of localization implemented.

A number of localization schemes exist to determine the location of a source object in relation to a reference coordinate frame. The vast majority of these depend on either acoustic or radio signals produced or received at some known location, which are then interpreted by various processing methods to extrapolate desired position data. Commonly, time of arrival (TOA), time difference of arrival (TDOA), and differences in received signal strength (RSS), or angle of arrival (AOA) between multiple nodes or multiple transmitters provide distances that can be converted into relative position through simple trigonometry. Yet, these methods are far from error free. The first issue lies in disruption of the required signal. Both radio waves and acoustic signals are subject to reflection, refraction, absorption, diffraction, scattering, or (in the case of mobile systems) Doppler shifts that may result in the introduction of non-trivial error [9]. Moreover, in real world situations, either intentional or coincidental conditions can lead to low signal-to-noise ratios in the desired medium, which will compound any instrument errors.

One of the most pervasive localization systems is the global positioning system (GPS) which uses radio signals and a satellite network enable worldwide localization. However, current high-precision systems are not available in a form factor (weight and size) that is appropriate for the specific limitations of a small quadrotor UAV.

Alternatively, many autonomous vehicles use inertial guidance systems (IGS) in navigation. Inertial guidance systems record acceleration and rotation to calculate position and orientation relative to a point of initial calibration. However, the system becomes increasingly inaccurate as time progresses and sensor error accumulates. Similarly to the GPS, reductions in size and weight result in unacceptable inaccuracies. Once again, we are forced to consider additional options.

A less-commonly used technology for UAV-specific localization is computer vision and video processing. While computer-vision based localization systems have been in use throughout the history of robotic systems, it was only in the past decade that this technology has come to widespread use. This likely occurred because of the recent availability of powerful open-source vision-processing libraries. For instance, Utilizing 2-dimensional, high-contrast tags containing unique patterns (see Figure 5: Sample A. R. Tag Patterns), special visual processing software can allow objects to be tracked in real time. By detecting the tag's edges and analyzing the perspective view and dimensions of the tag in the frame, the precise location and orientation can be computed [3]. Visual based tracking has the advantage of rapid updates, and will not be restricted by overhead obstacles. Moreover, because surveillance UAVs are, by the requirements of their task, already outfitted with the necessary optical equipment, computer vision promises to be well suited to the specifics of our project.

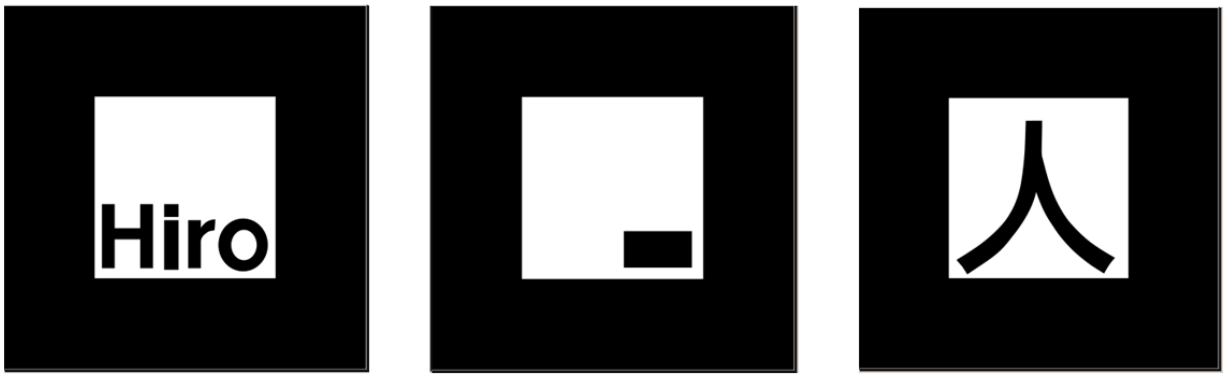

FIGURE 5: SAMPLE A. R. TAG PATTERNS

2.5 PREVIOUS PROJECTS

A number of projects from various research institutions have been conducted with varying levels of success in the area of UAV computer-based vision and object tracking, many of which are of interest to this project. Some of the most notable, applicable projects follow. We explored a number of previous research projects in the field of quadrotor UAVs, navigation schemes, control implementations, and potential applications. These projects helped to form a basis for our continued research. Several of such projects are summarized below.

2.5.1 UNIVERSITY OF TÜBINGEN:

Using the AsTec Hummingbird Quadrocopter, researchers at the University of Tübingen have set out to create a quadrotor system that is able to fly autonomously, without connection to a base station. They have outlined a number of areas in which research is required to complete their overall goal: flight control, lightweight solutions, three-dimensional mapping and path-finding, and vision-based self-localization.

The process involves low-cost, lightweight, commodity consumer hardware. Their primary sensor for the UAV is the Wii remote infrared (IR) camera (informally known as the Wiimote), which allows robust tracking of a pattern of IR lights in conditions without direct sunlight. The Wii remote camera allows position and orientation relative to the IR beacons on the moving ground vehicle to be estimated

The data returned from the Wii remote camera contains position of the four IR beacons in the camera frame, as well as intensity. This represents a clear example of the perspective-n-point problem (PnP). The use of IR, however, is impractical in the real-world, outdoor environment. We will utilize similar programming, but using a different form of vision to obtain the same data [10].

2.5.2 CHEMNITZ UNIVERSITY OF TECHNOLOGY:

Utilizing the Hummingbird quadrotor, researchers from Chemnitz University of Technology designed a UAV system that is able to take off, navigate, and land without direct human control, particularly in environments and scenarios when GPS data is unavailable or too inaccurate. They realize that a system that is robust and reliable enough for everyday use does not yet exist. They seek to design and create a robustly recognizable landing target, an efficient algorithm for the landing pad detection, a sensor configuration suitable for velocity and position control without the use of GPS, and a cascaded controller structure for velocity and position stabilization.

These researchers recognize one of the major problems of target tracking systems on UAVs: visibility of the target. If the target is too small, it cannot be identified from longer distances, thus rendering the vision system useless. Additionally, if the target is too large, the camera cannot fit the entire image in frame during closer-range flight. Our work with augmented reality tags will encounter the same problem with vision over varying distances.

To resolve this issue, the research team determined that their target had to be unique, but still simple enough to be tracked at a high frame rate. They used a series of white rings of unique widths on a black background so that the rings might be uniquely identified. Because each ring is indentified individually, the target can be identified even when not all rings are visible.

FIGURE 6: CHEMNITS QUADROTOR TARGET

The Chemnitz team, however, conducted the experiment as such that the landing target was on flat, stationary ground. Additionally, they assumed that the UAV was always perfectly parallel to the ground. If it was not, they used the internal inertial measurement unit (IMU) to provide adjustment. We seek to perform all position calculation based entirely on the vision system, with no aid from other sensors [11].

2.5.3 J INTELL ROBOT SYSTEMS:

Another project, completed by J Intell Robot Systems, also implements the Wii remote IR camera for visual tracking on a UAV. Their objective was to use inexpensive hardware to control the UAV with solely onboard processing. This project involves having a miniature quadrotor hover in a defined position over a landing place, similarly to our project's end goal for

localization. This project, however, uses the IR camera to calculate distance (or *z* position) and the yaw angle and uses the internal guidance system (IGS) to estimate relative *x* and *y* positions. These researchers focused on hovering at distances between 50cm and 1m from the landing platform using four IR beacons. Our team, however, will localize the UAV entirely based on the vision system at greater distances to demonstrate a more realistic application [12].

2.5.4 INSTITUTE OF AUTOMATIC CONTROL ENGINEERING:

At the Institute of Automatic Control Engineering, researchers completed a project that sought to use an onboard vision system, combined with the internal IMU, to hover stably at a desire position. This system uses a series of five markers of different shapes and sizes to determine the *z* position of the UAV, as well as the yaw angle. Again, the *x* and *y* components are determined by the IMU and the pitch/roll angles [13].

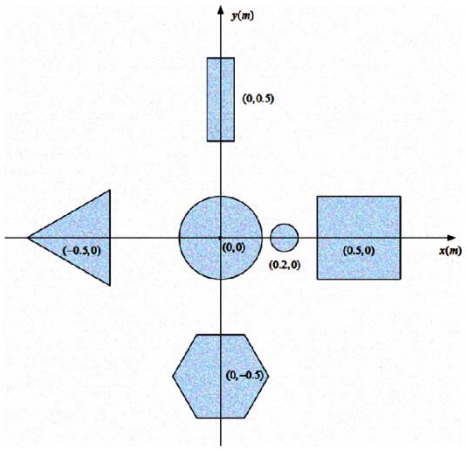

FIGURE 7: SHAPE-BASED TAG

2.5.5 RESEARCH CONCLUSION

Many of these projects attempt to solve the UAV localization and landing problem, often with methods similar to our own. This MQP, however, differs, as it puts a higher emphasis on the following:

- Purely vision-based localization, utilizing Augmented Reality Tags
- Support for localization between the UAV and a potentially moving target
- Recognition of real-world scenarios (distance from target, light conditions, relative velocities of objects)

3.0 METHODOLOGY

Our overall goal was to provide Lincoln Laboratory with a functional UAV system upon which they may expand in the future. To provide a strong foundation for further development, we set three goals; the completion of which would signify a successful project. Our project sought to: 1) create a functional PC-UAV control interface to allow commands to be sent to the CyberQuad, with relevant sensor data being returned when requested, 2) establish a localization scheme sufficient to operate the quadrotor with a high degree of accuracy in the 0-5ft range, and 3) provide clear documentation of our development process and the UAV's operation for the staff at MIT Lincoln Laboratory. Each goal represents a smaller sub-project with its own procedures, specifications, and results. In this chapter we discuss these sections of the project individually.

MIT Lincoln Laboratory envisioned this project as a springboard for future projects with quadrotors and desired that we demonstrate the abilities or potential of the system. The final product served as a proof-of-concept for quadrotor applications. We determined that the final demonstration would include the following:

- A functional interface between ROS and the CyberQuad's software
- Tele-operation of the CyberQuad via a ROS-controlled joystick
- A functional Augmented Reality localization system using an external camera
    - Movable camera in varying positions/orientations relative to the test-bed
    - Real-time, precise position/orientation knowledge feedback
    - Basic position-holding control-loop using constrained quadrotor setup

GENERAL DEVELOPMENT STRATEGY

To better manage this complex project and deal with the uncertainties that we foresaw in the early stages of development, we decided to follow a parallel path, iterative design process.

Because of our short development period, we understood the potential complications that could have arisen if we attempted to follow a linear development timeline. By dividing our project into three separate sub-projects, one for each of our three goals mentioned above, and focusing on specific iterations, we hoped to avoid the bottlenecks caused by a minor problem in one section of development. As such, if a problem were to occur with the control interface development, we would still be able to show progress in the localization scheme. Properly divided, this project provided sufficient work to keep each member of the project busy on a completely independent task for its duration. Each team member was charged with taking the lead role in one aspect of the project, but also helped in other areas to provide a different perspective on difficult problems.

3.1 DEVELOP PC CONTROL INTERFACE

SCOPE

The CyberQuad system, running the open-source MikroKopter control code, was originally intended to be operated by remote control or by pre-programmed routes programmed with a MikroKopter control program such as *QMK-Groundstation* (Linux) or *MikroKopter-Tool* (Windows). The first logical step in establishing a framework for future autonomous quadrotor applications was to devise a method for the programmable control of the system. If we were unable to use a PC to directly interface with the CyberQuad's MikroKopter hardware, we would not have been unable to accomplish the more sophisticated goals of the project – including integration with ROS. Lincoln Laboratory determined that this CyberQuad system (and MikroKopter hardware) is the platform they will be using in future, and standardizing moving to a standard control system would facilitate accelerated collaborative development moving forward.

We determined that the most logical method of communication to the quadrotor from the PC was to utilize the MikroKopter hardware's serial debugging port – the same connection used by the stock MikroKopter control utilities, such as *QMK-Groundstation*. This serial link, when connected via a wireless serial adapter, would therefore provide a simple method for communication between the PC and quadrotor.

Below, Figure 8 shows the conventional communication methods with the CyberQuad – a handheld transmitter and pre-programmed waypoints.

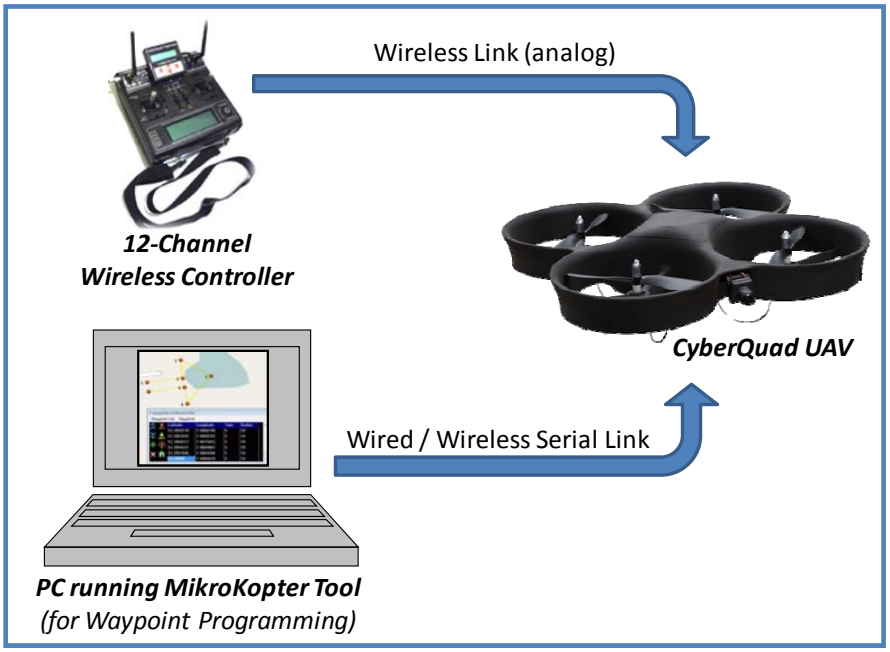

FIGURE 8: CONVENTIONAL MIKROKOPTER CONTROL METHODS

Figure 9 represents the designed communication scheme that we planned to implement. It allowed communication by handheld wireless transmitter, pre-programmed waypoints, ROS joystick, and wireless PC control.

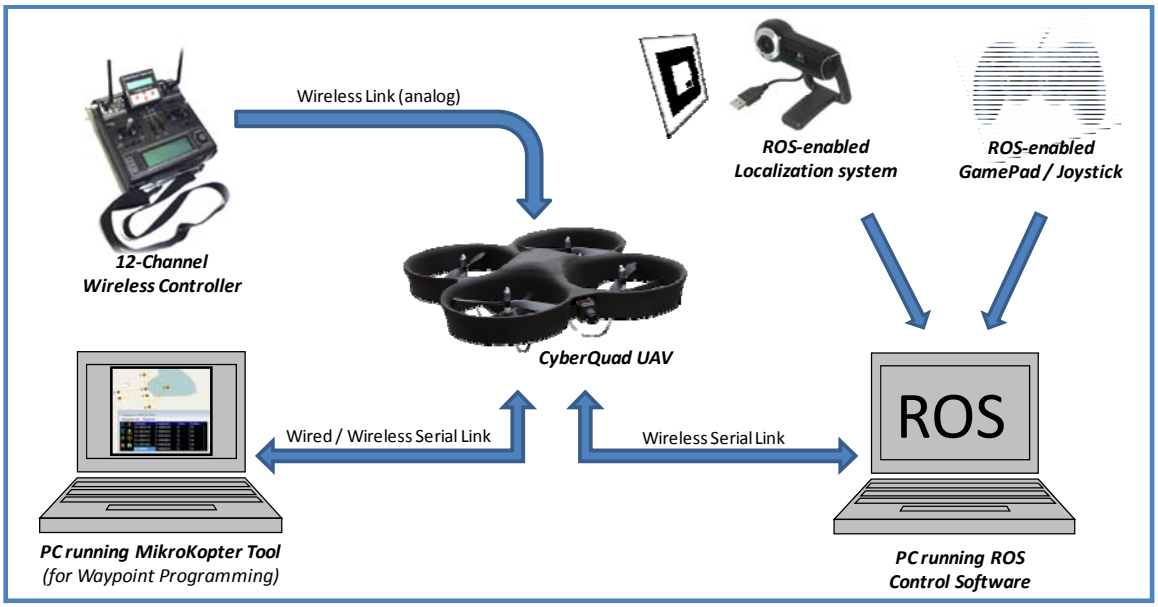

FIGURE 9: OUR PROJECT'S IMPLEMENTED CONTROL METHODS FOR THE MIKROKOPTER

3.1.1 DESIGN SPECIFICATIONS

The PC control interface needed to meet a number of requirements to demonstrate its success. These specifications, determined in the proposal phase of the project, served as guidelines for system's development. They are as follows:

- Our system must be able to pass commands to the MikroKopter hardware from a ROS node (with demonstration via a ROS joystick).
- The UAV adapter must provide a level of abstraction sufficient to offer Lincoln Laboratory engineers the ability to communicate with the quadrotor in a form that is more convenient than by forming low-level MikroKopter serial commands.
- The UAV adapter should provide visibility for all messages passed by the system. ROS offers two available options for inter-nodal communication: asynchronous publishing/subscribing and synchronous request/response. The publisher/subscriber sub-system allows for detailed logging and playback of all messages passed. Our system must employ this asynchronous system because the messages are visible to ROS logging

tools, while synchronous communication messages are not. This implementation will ensure that the UAV can be operated by both high-level command nodes as well as at the low level via the command prompt.

- Given the time constraint, our system must first implement functions for passing only the most important messages. The adapter must be able to send basic movement-related controls, receive navigation data, and overall ensure functional, extendible serial communications. The serial communication test should be used to test the system for functionality.
- The serial communication scheme must feature multi-threading to ensure simultaneous read/write functionality.

3.1.2 DESIGN DECISIONS

Before any coding began, we dedicated a significant portion of time to designing a control system architecture that was appropriate for the task at hand. This helped to break up the complex task of developing the quadrotor interface into more manageable components. Furthermore, with well defined interfaces within the system, multiple individuals could work on the same project in parallel without having to wait on the completion of one section to start another.

INITIAL DESIGN

Creating a CyberQuad control interface began with research regarding the two software and hardware systems to be interconnected. We studied the existing MikroKopter hardware and software of the CyberQuad, as well as ROS documentation and sample ROS systems. Our focus was initially towards determining methods by which to exploit any existing message-passing systems in the MikroKopter hardware and software. In particular, we intended to use the quadrotor's serial message protocols to provide navigation-related feedback and flight control.

In our research, we discovered that there already existed a several relevant software projects on the topic of serial communication schemes. Within the ROS library, there were several simple examples of serial communication nodes. Likewise, the pre-existing diagnostic and command tool for the CyberQuad, *QMK-Groundstation* (the MikroKopter ground-control center software for Linux), made use of the serial communication protocol. While neither project fit perfectly into our program specifications, a combination of the two provided a solution to the task of establishing PC-UAV communication.

The next step in the design of our project was to determine the level of abstraction presented to the user of the control system. The *interface* concept was applied to the CyberQuad, with the system providing an abstraction of the lower-level processes so that Lincoln Laboratory researchers would be able to operate the UAV with simple, high-level commands, rather than the complex low-level, ambiguous serial commands made available by the MikroKopter software. Taking advantage of ROS's simplified multi-process communication system, a layered interface approach could be used in the development of the system. Once the lowest level communication node was created, additional interface nodes could be layered on top of this and each other, each providing a higher level of abstraction to the user than those it builds upon. As such, the abstraction level could become increasingly higher-level as the system undergoes development in the future.

To initiate this abstraction, we chose to first develop what we called an "adapter" - a system providing the ROS-topic API to the to the low-level MikroKopter serial commands. This would hide the low-level serial protocols and processes, only providing user-access to more user-friendly commands and data. The physical data stream between the devices would only be handled internally, as it is not immediately important to other elements in the ROS system. The adapter we developed will allow researchers at Lincoln Laboratory to record, analyze, and repeat the messages passed over serial communications, with the messages remaining in a human-readable format.

A functional adapter system required multiple processes running simultaneously to accomplish the tasks at hand, namely: sending commands through the serial port, receiving serial responses, and monitoring the link between the PC and the quadrotor. The two main possibilities for the structure of the ROS-MikroKopter communication were: 1) a system multiple ROS nodes to emulate the required "multithreading" capabilities, or 2) employ actual C++ multithreading in a single ROS node to accomplish all of the tasks. Clearly there are advantages and disadvantages to both methods, particularly with regard to our previous experiences – a high degree of C++ experience, with no ROS background - and to the task at hand. Given this, our first design developed into a single, monolithic C++ program encapsulated within a single ROS node, as pictured in Figure 10. Moreover, this implementation would have clearly fit the standard definition of an "interface", in that it provides functionality to a user through a defined API, yet hides all the implementation that provides the functionality. Likewise, it would minimize inter-ROS node communication, as the user API could be defined to have only a few, simple commands. Though it was against the message visibility guidelines, we initially planned to use a request/response system for any communications that needed to occur, as it often simplified the implementation.

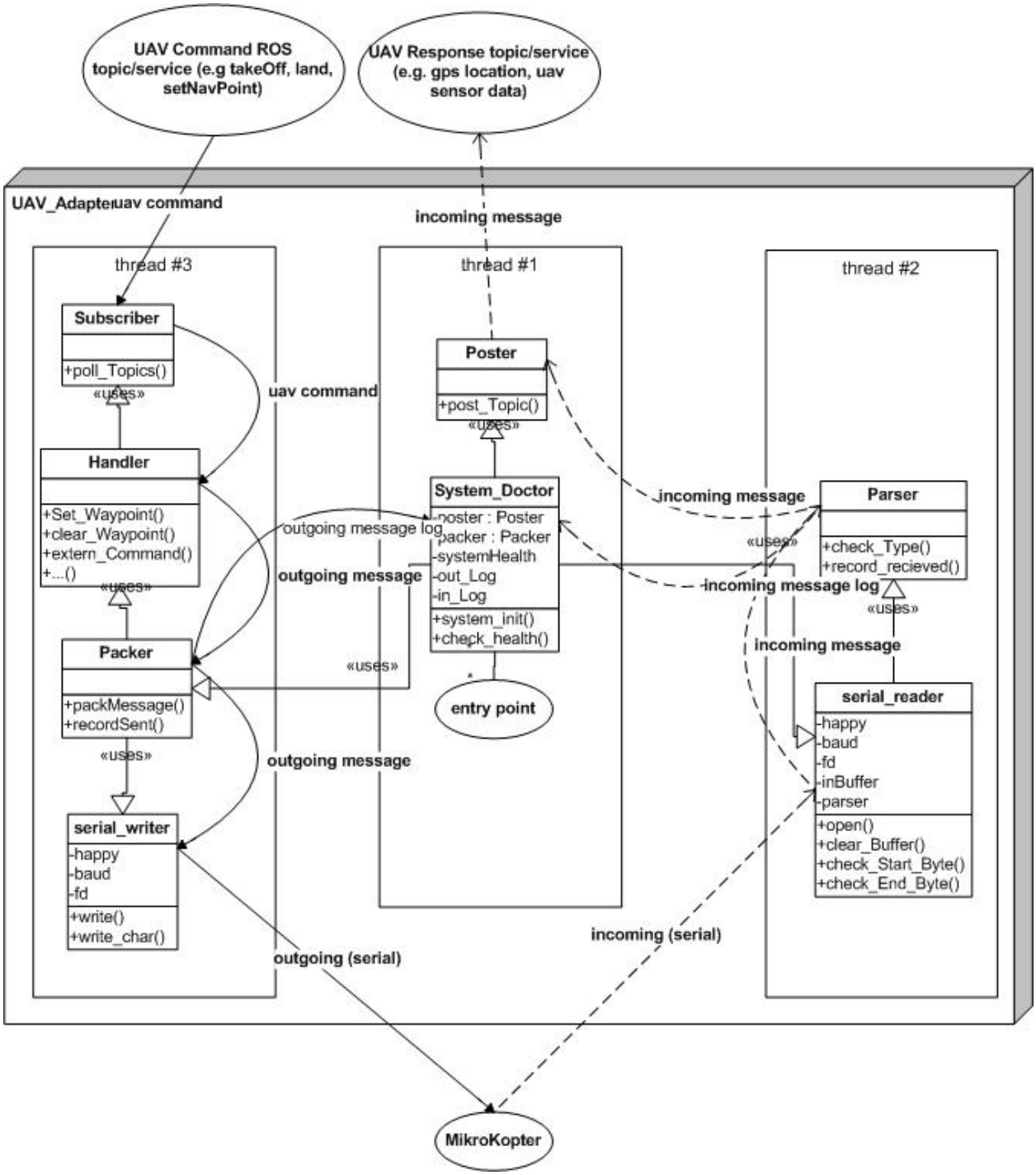

FIGURE 10: UAV_ADAPTER MONOLITHIC DESIGN

FINAL DESIGN

Following the initial project proposal presentation, we changed our software architecture to more readily accommodate the desires of MIT Lincoln Laboratory. The new configuration is shown below in Figure 11. The ROS-distributed system required message passing in the form of visible “topics” that were visible throughout the entire ROS system. This implementation more clearly fit our design specifications, and was therefore, the optimal choice. The primary motivation for changing our system, however, was to enable greater low-level visibility. Our project would be used by Lincoln Laboratory after its completion and the Laboratory engineers required visibility access to the serial communications for the purposes of logging and repeating experiments and procedures. This new philosophy helped to create an “adapter” that would allow for complete and unmodified access to the MikroKopter protocols through ROS, rather than a true system interface for the CyberQuad system. The original monolithic C++ structure was divided up into several ROS nodes that communicate via topics (rather than request/reply services), as seen in Figure 12.

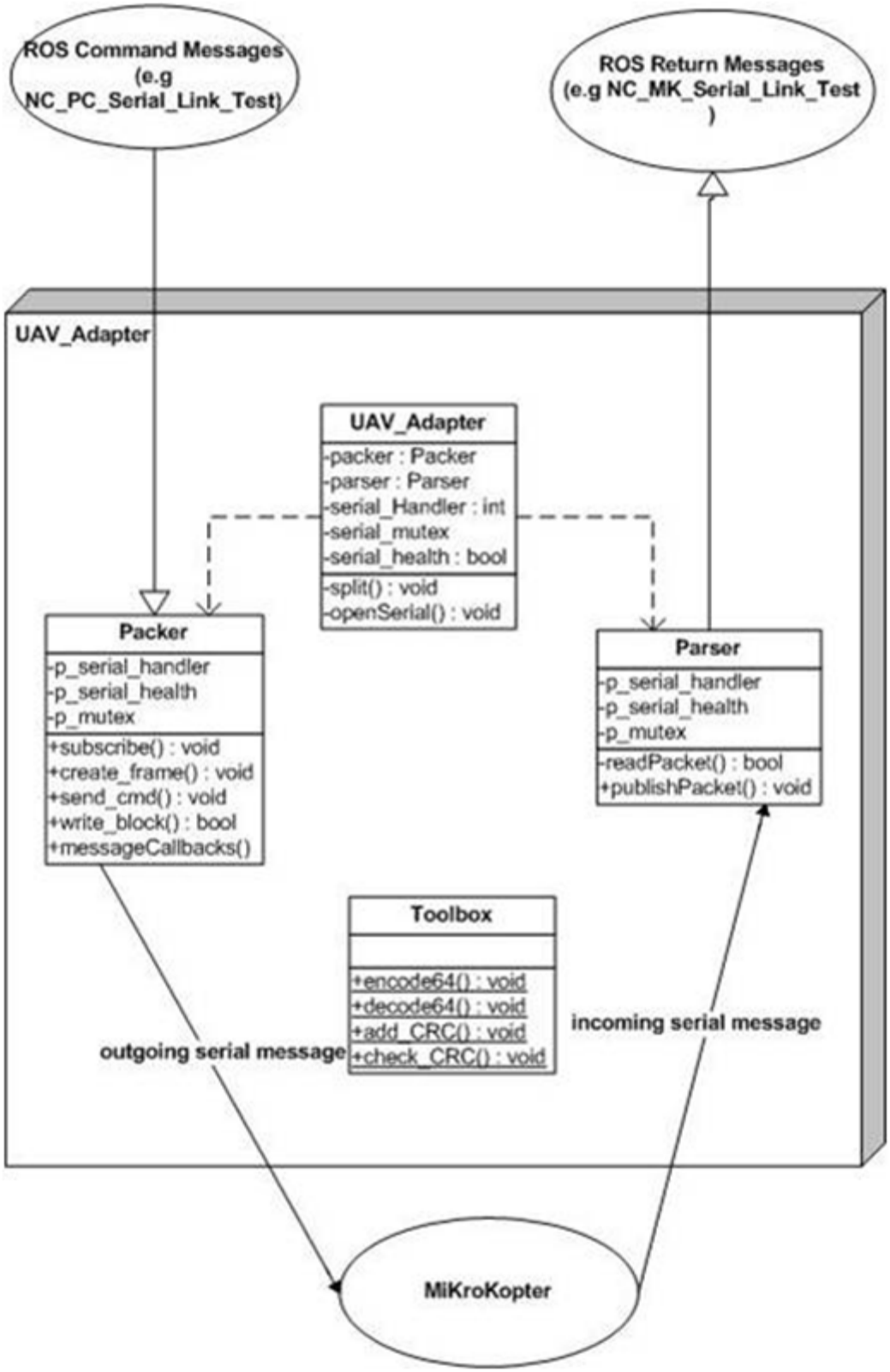

FIGURE 11: UAV_ADAPTER FINAL STRUCTURE

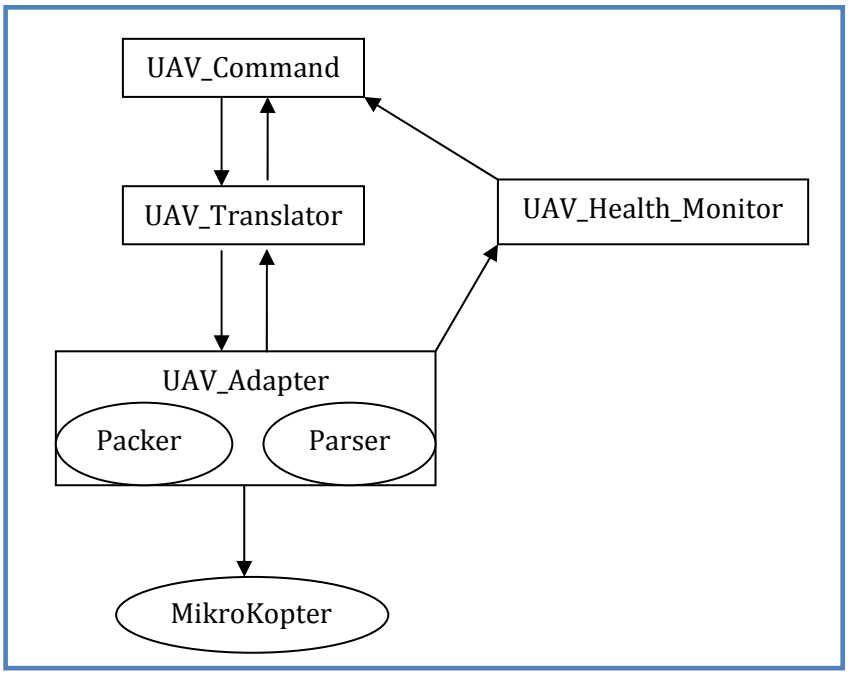

FIGURE 12: ROS NODE CONFIGURATION

In our design, there were three ROS nodes placed at varying system levels. The lowest level ROS node was the *uav_adapter*. The purpose of this node was to handle all of the serial port communication between the CyberQuad and the PC. The *uav_adapter* subscribed to ROS topics and translated those messages into MikroKopter-compliant serial messages. It also received messages over the serial link and converted those messages back into ROS-compliant messages. The *uav_adapter* then posted the ROS messages to the appropriate ROS topics for use in other parts of the system.

The connection to other ROS nodes was divided into two broad categories: command-type and the return-type messages. The command type included a topic for each command in the MikroKopter serial protocol. The returned message type includes a topic corresponding to each message returned from the MikroKopter serial protocol.

The next ROS node in the system hierarchy was the *uav_translator* that was designed to translate higher-level ROS messages into a more complex set of low-level MikroKopter commands, as well as provide an abstraction layer for the sensor returns. Though this node

would never be fully implemented for this project, it would provide the framework where future developers could create simplified commands. In the simplified version used for this project, this node would subscribe to a higher-level command node and pass messages to the *uav_adapter*, then receive the *uav_adapter*'s return messages to be passed upward, acting as a pass-through.

Finally, the highest level node was *uav_command*, providing the application-level programming for the UAV control system. This node served to implement some degree of automated control of the UAV. This way it served both as a means to test existing code and a placeholder for future high-level development.

Another ROS node was created in parallel to this message-translation system: the *uav_health_monitor*. This node subscribed to one ROS command message and one MikroKopter returned message that existed to test the serial link. It compared the sent and received messages and generated a metric of link health and latency, posting the results to a separate topic.

3.1.3 DEVELOPMENT

Development of the UAV adapter system involved developing a series of independent ROS nodes, with different levels of abstraction. We were able to decompose the development process to allow each node to be developed individually and simultaneously, and in some cases, to enable simultaneous development of different elements of the same node. While one team member worked on the serial communication, another was able to work on the non-serial components of each ROS node – some of which did not even require serial communication to fully develop. Each component was developed iteratively, often beginning with example code from ROS or the MikroKopter QMK-Groundstation source code in early iterations. After a sufficient understanding was achieved, the code was re-written to more accurately meet our

goals. In this section, we explain the development process for each of these major components of the UAV adapter.

SERIAL PROTOCOL

In an effort to save time in the development of the serial communication code, we modified existing code to serve our purpose. While researching potential pre-existing ROS nodes with serial components, we came across the ROS *serial_port* package. For some time, we discussed the merits of using this seemingly functional system. Ultimately, we decided that modifying the *serial_port* package as a ROS node would create too much overhead, in the form of unnecessary ROS messages, and additional latency because every message would have to travel through multiple sockets. Moreover, we anticipated that attempting to modify this code to be multi-threaded would take longer than developing the multi-threaded system on our own. Although all ROS node support multithreading through the Boost library which is included in the core ROS library, by rewriting the *serial_port* package we would have had the greatest control over the multithreaded behavior and shared serial port resources.

Although the decision was made to not use the *serial_port* package as a self-contained system, we repurposed a significant amount of the C++ source code. The first issue we encountered during the serial development portion was the inability of our operating system (Ubuntu 2.6.13) to recognize the MikroKopter debug board (MK-USB) as a TTY device. However, to test our code, we connected two PCs together via serial crossover cable with one PC using our serial code to generate serial data and the other PC receiving the serial data in a terminal window.

Eventually, we found a solution by which to accomplish serial communication across the MKUSB. By removing the default Ubuntu package *brltty*, a package designed to allow for Braille hardware interfaces, we were able to open the *ttyUSB* port corresponding to the MK-USB board with both read and write capability.

Once the serial port was open, we began testing our serial code with simple MikroKopter commands. During these early tests, however, communication only functioned in one direction; we sent messages to the quadrotor, but could receive none of the expected return messages. We employed the QMK-Groundstation software recommended by the CyberQuad developers, other example serial code, and a direct electrical analysis of the serial port using an oscilloscope to determine that the fault in the communication was a result of a faulty UART connector.

With a working connection, we began developing the correct MikroKopter message frames that would allow for bi-directional communication to the quadrotor. Each MikroKopter message was formed by a start byte, a destination address byte, message ID byte, a variable length payload, a two byte checksum, and an end byte. We employed previous MikroKopter communication projects in order to accelerate our development of these messages, particularly QMK-Groundstation, the Linux equivalent to CyberQuad's default debugging software suite. QMK-Groundstation received feedback from the MikroKopter sensors, performed engine tests, and configured low-level settings.

Our message generation development involved simple tests to ensure that communication between the computer and MikroKopter was functional - sending small, well-defined messages which provided consistent return values. We manually encoded these messages into a buffer to be sent to the quadrotor using our serial handling code. Our communication code successfully sent messages over the serial link to both run the engines in test mode and to trigger system version responses. The next step in development required the ability to send messages that carried a higher data payload, as these test messages carried very little data.

MikroKopter's serial protocol specifies a modified 64 bit encoding scheme, which was handled correctly by QMK-Groundstation by using the Linux *Qt* libraries. Our code, however, lacked the data types and operations provided by Qt. Therefore, we had to address this encoding ourselves to properly encode these messages. In MikroKopter's encoding scheme, valid payload

characters range from '=' (decimal 61) to '}' (decimal 125). Although never explicitly explained in the English pages of the MikroKopter Wiki, it seems that this scheme is implemented to prevent payloads from inadvertently containing frame starting or ending characters ('#' decimal 35 and '\r' decimal 13). Table 6 presents an example of MikroKopter's encoding system that we addressed in our serial code.

TABLE 6: SIMPLE BASE64 COMPUTATION

Original value	A (decimal)	B (decimal)	C (decimal)
Offset value (n)	a (decimal) = A + n	b (decimal) = B + n	c (decimal) = C + n
Bit representation of new value	$a_7a_6a_5a_4a_3a_2a_1a_0$	$b_7b_6b_5b_4b_3b_2b_1b_0$	$c_7c_6c_5c_4c_3c_2c_1c_0$
Base 64 representation	$00a_7a_6a_5a_4a_3a_2$	$a_1a_0b_7b_6b_5b_4$	$00b_3b_2b_1b_0c_7c_6$	$00c_5c_4c_3c_2c_1c_0$

We addressed, and compensated for, the encoding difficulties that arose because the data payload was expanded in such a way that the encoded serial payload was no longer consistent with the size specifications in the MikroKopter serial protocol documentation. For example, a serial link test pattern was specified to have an unsigned 16 bit (2 byte) payload. When expanded to base 64, however, the true message becomes 4 bytes - twice the anticipated data length. Without properly accounting for this change, data payload was incomplete and misinterpreted, and checksum generation was often incorrect; these incorrect messages were often ignored by the MikroKopter.

ROS NODES

The UAV adapter system required a number of different ROS nodes to accomplish all of the functionality established by the design specifications. These nodes were constructed in a hierarchical structure to fit the needs of the final system. Figure 13 shows the ROS system

configuration created for the operation of the CyberQuad. The arrows demonstrate the directions of communication between the nodes. The *uav_msgs* node does not communicate with any of the other nodes, but it supplies message definitions to all of them. Additionally, *Joystick_Ctrl* was not created specifically for the quadrotor; it is a commonly-used ROS node that was adapted to operate with this particular hardware and project.

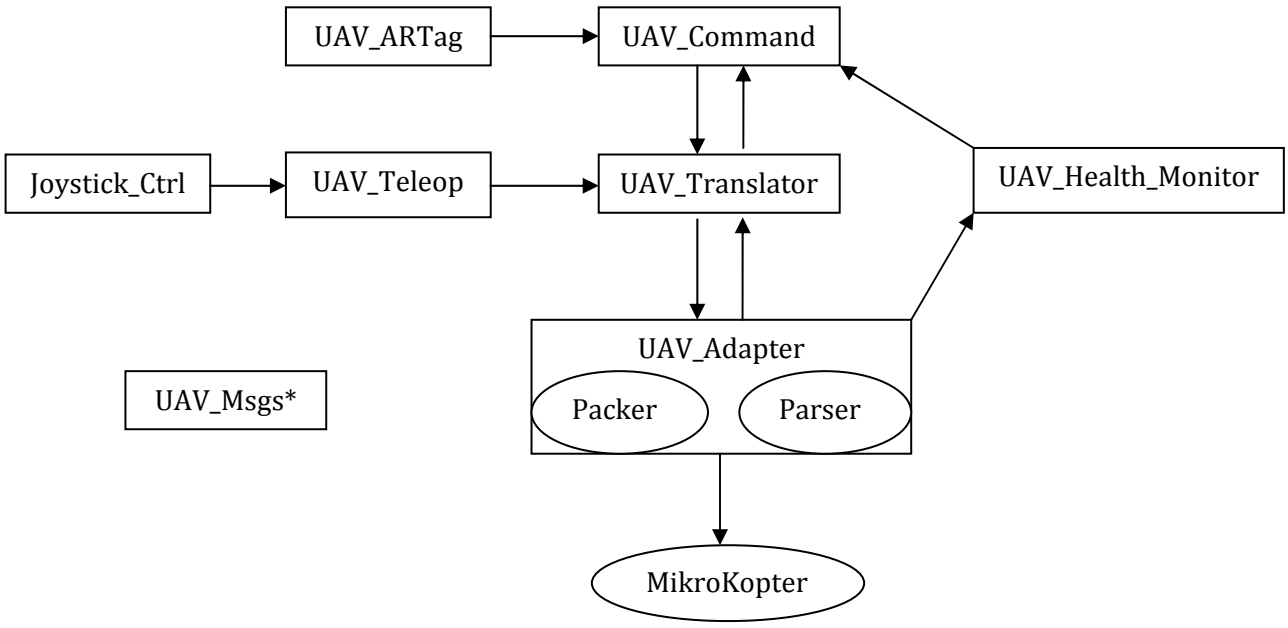

* This node contributes to every ROS node, but doesn't directly communicate with any.

FIGURE 13: THE CYBERQUAD'S ROS CONFIGURATION

uav_adapter

The *uav_adapter* involved three different classes to perform the multithreading functions of serial I/O for which this node was designed. The first class, the *Packer*, subscribed to messages from a node higher in the hierarchy of the UAV adapter system, converted the messages to a MikroKopter-compatible format, and sent those messages over serial to the quadrotor. The second class in the *uav_adapter* was the *Parser*. This class received returned serial messages from MikroKopter, parsed those messages back into a ROS-readable format, and published them back into the ROS system. The final class was the *UAV_Adapter* class that

provided the constructors and destructors for the *Packer* and the *Parser*. Each of these classes was developed individually due to their independent functionality. This division of the *uav_adapter* into separate objects allowed all the group members to work effectively in parallel.

The first step in developing the *uav_adapter* was to establish the base class, *UAV_Adapter* to handle the constructors and destructors of each thread. In the early stages of development, we created placeholders for the constructors of the *Parser* and *Packer* to ensure that each thread was instantiated correctly. Initial development of multithreading began with the creation of a method in the *UAV_Adapter* class that called separate methods to instantiate the *Packer* and *Parser* as separate threads using the *boost::thread* method. To confirm that the multithreading was working properly, the constructors in the *Parser* and *Packer* were temporarily configured to continuously print status messages. Be viewing the output of the *UAV_Adapter* class's execution, we were able to confirm that several threads were executing simultaneously and functioning correctly.

Once the serial communication code had been implemented, revisions were made to the *Parser* and *Packer* constructors to allow for references to shared resources to be passed into the object to allow for simultaneous use of the serial port. Additionally, a *boost::mutex* object was created in the *UAV_Adapter* class, to which both the *Packer* and *Parser* were provided access. By locking and unlocking this mutex around critical sections in the executed code, the shared serial resource was protected. The *Packer* served to write to the serial connection, while the *Parser* performed all read functions simultaneously.

In the *Parser*, we developed a state machine that received a series of data characters from the incoming serial buffer and reconstructed them into a full message. Based on the known start and end bytes of the MikroKopter serial protocol and the checksum analysis code from the QMK-Groundstation, we determined the difference between correct and corrupted messages. The *Parser* would then publish these reconstructed ROS messages to a node higher in the UAV system hierarchy.

For the message reconstruction code, we created a set of structures for the relevant MikroKopter messages to be copied into. This way, we had access to specific fields of a message by first casting that message into a general structure. Once the data fields of a received MikroKopter message were all processed, the information was inserted into a ROS message structure and posted to the appropriate ROS topic.

The *Packer* was constructed in a similar manner. In its idle state, it continuously polled the topics to which it subscribed for new messages from other nodes in the hierarchy. When it received a message, it triggered a callback function that created a message with the required MikroKopter message ID and populated the outgoing message with the proper data fields. Then the message was sent over the serial link to the MikroKopter.

To ensure that the entirety of the system was functioning as a whole, we had a separate ROS node, the *uav_health_monitor,* send out MikroKopter echo packets. These messages were interpreted by the *Packer*, triggered in the correct callback, packed into the correct data frame, and sent over the serial to the MikroKopter hardware. The MikroKopter generated a response message and returned it over the serial link. The *Parser* then reconstructed the message byte-by-byte, and forwarded the correct message back into the UAV system. The *uav_health_monitor* listened for this return message, and determined if messages had made it around the full loop to the MikroKopter and back.

uav_translator

The *uav_translator* node was originally designed to act as an abstraction layer converting higher level commands to low-lower level (such as those used by *uav_adapter*). For this project, it served a slightly different purpose, simply re-routing messages from other nodes to the *uav_adapter*. Additionally, this node received return data from the MikroKopter after it has been read from serial, parsed, and sent as a MikroKopter-returned ROS message from the *uav_adapter*. This node was also designed to receive these return messages, translate them into

a more usable, higher-level message, and post them to topics readable by nodes higher in the hierarchy. Figure 14 demonstrates an example of the proposed functionality of this node, if it were implemented as desired for the final design. The messages employed by the *uav_translator* module are simpler, clearer, and more intuitive than the obscure MikroKopter protocols sent at the lower levels.

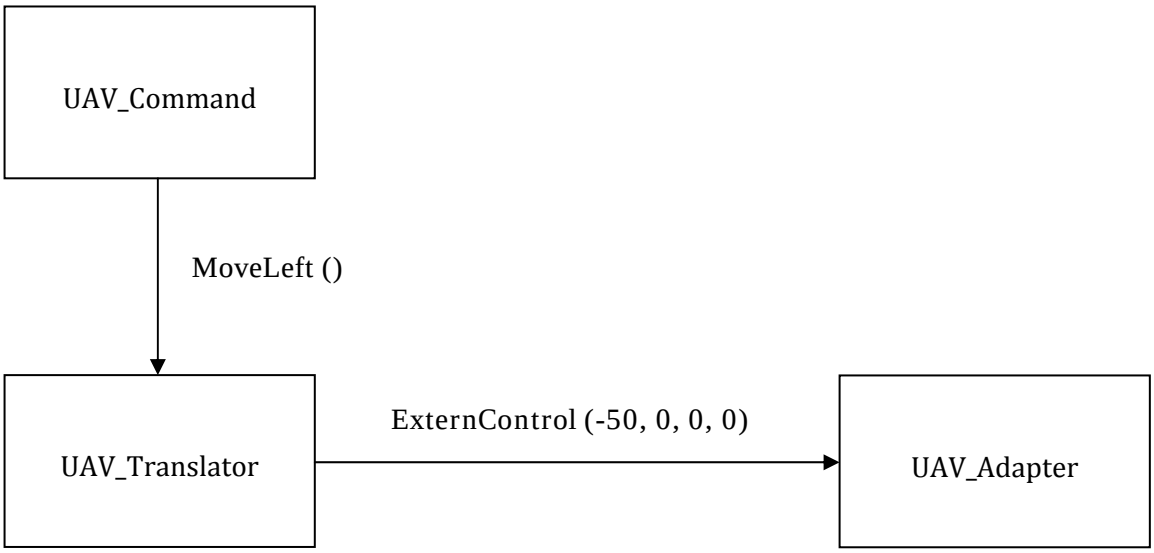

FIGURE 14: UAV_TRANSLATOR

Development of this node began before the formats of either the low-level or high-level messages were determined. The first iteration saw a simple implementation of the publish/subscribe feature, with the ability to post to all topics that carried a command to be sent to the MikroKopter, as well as to subscribe to all topics that contained messages returned by the MikroKopter. Work on this node was largely suspended for a majority of the project during the period when no return messages could be read from the quadrotor.

We realized, however, that we needed testing procedures to ensure that our code was operating properly once connected to the UAV hardware. We determined that the *uav_translator* should be used as a test suite for the low-level commands that we intended to implement. Because of its ability to pass MikroKopter commands directly to be packed and sent

over serial, this node worked well for testing. It published test messages and subscribed to the responses. This node contained none of the multithreading complications inherent in directly testing the *uav_adapter*, and it allowed for easy comparison between commands sent and responses received.

Finally, framework for adding high-level commands in the future was established. Several example messages were implemented in code, albeit not fully, though the framework has been established for use by future developers. In future iterations of this particular node, the number of topics the *uav_translator* publishes and subscribes to must be increased. At the completion of this project, the translator only published those messages that we found to be most relevant to providing the proof-of-concept system. Many of the minor functions of the MikroKopter serial protocol remained unimplemented in each translating, sending, and receiving.

uav_health_monitor

The *uav_health_monitor* was an addition to our adapter system to provide an indication about the state of the messages being passed to and from the CyberQuad system. In the first iteration of this node, it subscribed to all of the important message topics, both from the *uav_translator* and the *uav_adapter*. The *uav_health_monitor* implemented a linked list to store a queue of message times on the "sent" side of the *uav_adapter*. It would then assign message times coming from the "received" side of the quadrotor to a separate queue. Over a specified time period, the *uav_health_monitor* would build these queues, and at the end of that period, it would calculate the average latency over that time period, compare the number of messages sent to the number of messages received to determine link health, advance the queues, and clear old messages.

Figure 15 depicts the linked list employed by the *uav_health_monitor* to keep track of all messages sent and the time at which they were sent.

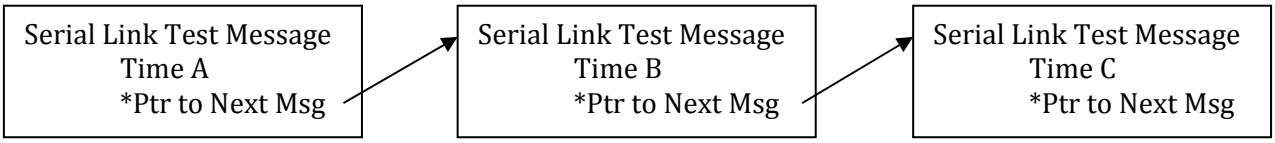

FIGURE 15: THE LINKED LIST OF SENT MESSAGES

Soon after development began, we realized an problem in our design. With the *uav_health_monitor* subscribing to so many messages, if a message were dropped, there was no way of knowing what message it was. Additionally, the queues of messages only stored a timestamp, and no other relevant data. Finally, this method provided only a sampling of link health; it would potentially fall very behind in the queues while it processed the data, advanced, and cleared the queues. We determined also that this implementation would take a significant amount of time to develop and test. This would likely require modifying the MikroKopter firmware to provide timestamps as a field on all return messages, for a full implementation.

After re-evaluating the *uav_health_monitor*, we developed an entirely different technique f or monitoring link health. This time, we used the built-in MikroKopter serial command *serial_link_test* to monitor the connection. The *uav_health_monitor* sent a message to the MikroKopter at a user-defined rate that carried an "EchoPattern," (an unsigned integer) and the quadrotor would return that same value. The queue was changed to store only the *serial_link_test* messages sent from the *uav_health_monitor* – their EchoPattern, or index#, and a timestamp. This message would be read by the *uav_adapter*, sent to the MikroKopter, and the response received. When the *uav_adapter* posted the return message, a callback function in the *uav_health_monitor* assigned the incoming message a "return time". It would then compare the index of the incoming message to the first message in the queue of sent messages. A mismatch implied a dropped message, and could be handled accordingly. Otherwise, the *uav_health_monitor* calculated latency based on the sent time vs. return time, as well as the link health based on the number of packets dropped over a certain time interval.

Figure 16 is the new setup of the linked list system that would keep track of both "EchoPattern" and the timestamp associated with both the incoming and outgoing messages. The messages returned by MikroKopter (through the *uav_adapter*) are not linked, as they are solely used to compare against the existing linked list, then discarded.

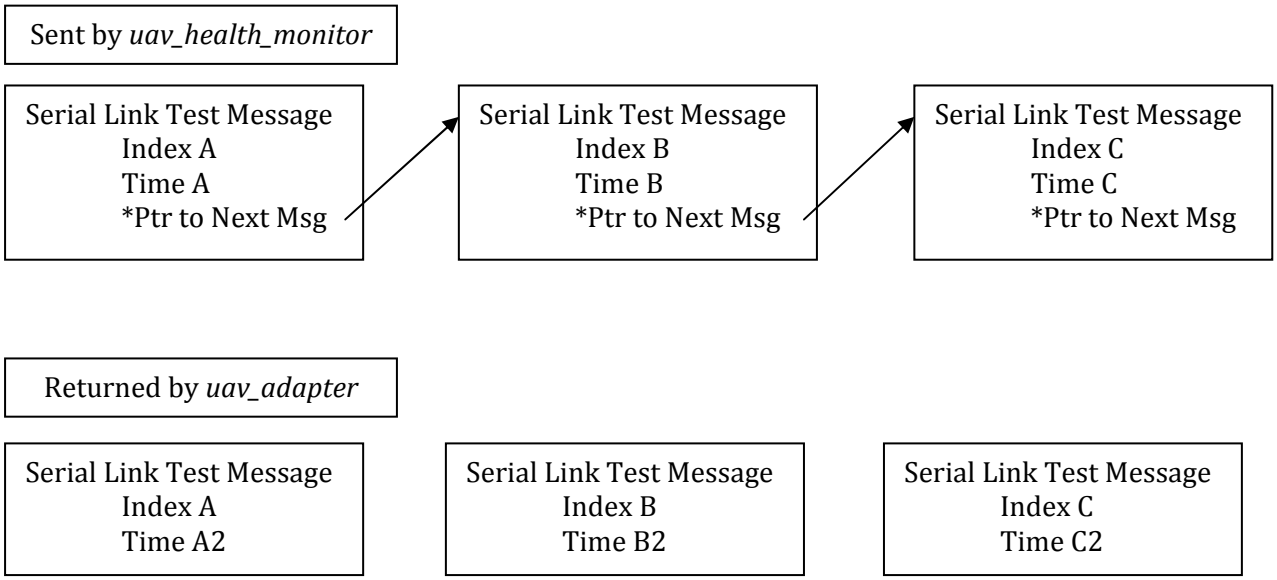

FIGURE 16: AMMENDED LINKED LIST SYSTEM

To improve on the old system, the new design updated latency and link health in a continuous, real-time manner, as opposed to the sampling method used previously. The updated *uav_health_monitor* employed a moving buffer that stores the result of each message callback; it stored a '0' for a successfully returned message, and a '1' for a dropped message. The link health was calculated over this set-length time interval, and when the buffer advanced, it cleared old results, as seen in Figure 17. This way, as time advanced, new dropped messages remained significant to the calculation of link health. Additionally, the latency of the link was calculated using a weighted average to ensure that the most present latency results were the most significant, but also so that there is some smoothing of the sampling, ensuring an outlier does not potentially provoke an overreaction from the subscribing quadrotor control nodes.

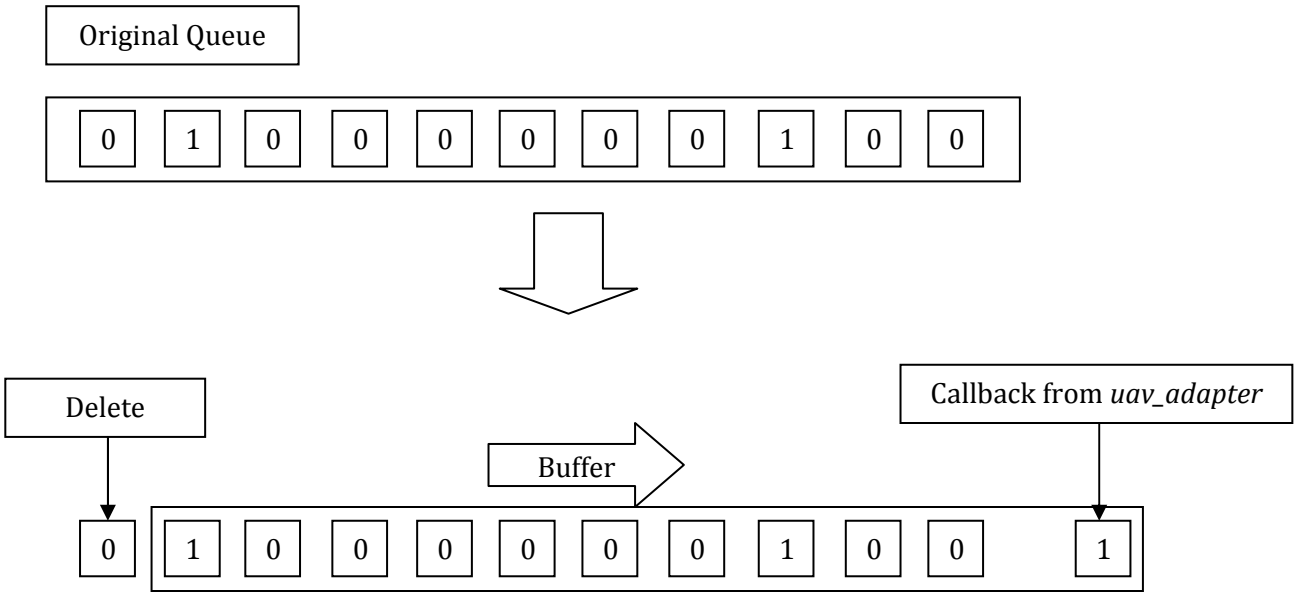

FIGURE 17: LINK HEALTH QUEUE CONTROL

In a late evaluation of this node's functionality, however, we noticed another shortcoming in its design. While the *uav_health_monitor* kept track of the number of dropped messages, latency, and link health, this information was only made available to other nodes when that information could be calculated (if and only if a response was received from the MikroKopter). If, for some reason, the link was disconnected, the user wouldn't necessarily be aware of the dropped connection because *uav_health_monitor* only publishes a message after receiving that response. Thus, we implemented a timing system to monitor the responses and ensure that a response is received every few seconds (the exact value to be assigned by the user). Otherwise, *uav_health_monitor* publishes to a separate topic that alerts any subscribers that the link is disconnected. Upon re-establishing connection, the node returns to normal operation.

This node was completed with all of the specified functionality. Additional functionality could be added to monitor another MikroKopter command, rather than having an entire publisher-subscriber topic just for testing the link health. In a more advanced quadrotor system, this extra *serial_link_test* topic might place unnecessary burden on the serial port that could be avoided by sampling the output of another message. The best possible alternative would be to

monitor the external command (which has a confirm frame similar to the serial test message) or the OSD data (navigational data returned from the MikroKopter at user-defined intervals) comparing return time to the expected return time as defined by one of the MikroKopter serial commands. For the purposes of our project and projects in the near future, however, this implementation was determined to be more than sufficient.

uav_teleop

This simple node serves to allow for ROS joystick (in this case, a dual 2-axis Logitech Gamepad) control of the quadrotor for the main purpose of testing. Many ROS-enabled robots at Lincoln Laboratory utilize this controller, and we felt it appropriate to adopt the same standard. Building off of ROS's built-in joystick control functionality, *uav_teleop* subscribes to the joystick node's output messages (in the form of two arrays: axis[] with one element for each joystick axis, and buttons[] with one element for each button on the controller). This node then converts these values into quadrotor-specific functionality for each axis and button.

Our joypad implementation features handling for two analog control sticks (altitude and yaw, pitch and roll) and four buttons. The first button enables the 'locking' of output thrust, meaning that you can set the UAV to a desired thrust using the control stick, hold this button and release the control stick and the UAV will continue to receive the same thrust. The second button acts as a scaling mechanism for the joystick axis in the event that the operator wishes to issue more precise commands to the quadrotor. For example, without the scaling, full left on the left control stick might make the quadrotor rotate at a rate of 1 radian/second. With the scaling button pressed, it would only rotate at a maximum rate of 0.5rad/sec. This function allows the user to adjust the control scheme in real-time for more precise maneuvers. The third button allowed for the re-centering of the thrust control stick. From our limited flight experience, we concluded that it was useful to have the default position of the thrust control stick to be the value that makes the quadrotor hover. However, because this value can vary substantially from

flight to flight, it could not be hardcoded into the software or even passed as a parameter on the launching of the ROS node. Instead we had this button take the current value of the thrust and adjust all subsequent values so that the new default value of the control stick was hover. The final button was simply a reset button, which reset the centered control stick back to its original configuration.

The *uav_teleop* node existed as a framework for future implementation. Though we did implement the essential control elements, we did not experiment with all of the MikroKopter's serial commands to determine if there were others that were valuable to implement on the controller. Future projects will likely find a number of additional uses for the buttons on the gamepad, and this node is designed to easily support adding new functionality.

uav_command

We developed *uav_command* as the central processing center for the quadrotor's operation. This node would operate above the *uav_translator* and *uav_adapter* in the hierarchy and pass high-level commands through the *uav_translator*. All sensory systems – AR vision, GPS data, sensor fusion, etc. – would be analyzed and combined in this node to determine the UAV's best course of action.

Due to time constraints, however, we were unable to fully implement all of the functionality for which this node was designed. Instead we created a framework for anticipated future applications. Additionally, we also programmed a number of test cases into the current version of the *uav_command* to demonstrate proof-of-concept and provide an outline for future developers.

One of the primary means by which to quantitatively measure the functionality of the UAV system as a whole was to write and retrieve data from a log file for analysis. We used the standard C++ I/O libraries and some file manipulation to output the results of the various

processes of the UAV system to comma separated value (*.csv) files for later analysis. Persistent data could now be saved outside of ROS for more extensive external analysis.

Additionally, in order to test our localization system, we created the means by which to specify an arbitrary 3D coordinate anywhere in space in respect to the augmented reality test tag and then calculate the difference between this "setpoint" and actual position of the UAV based on the localization data provided by *uav_artag*. To accomplish this error calculation, we made use of ROS's built-in frame transformation messages. Every time *uav_artag* detected an augmented reality tag, it would post the orientation and position data as a frame transformation. The *uav_command* subscribed to these messages, and would combine the incoming data with frame transformation information about the UAV's position in respect to the camera, upon receiving a message. This allowed for the construction of a ROS frame transformation tree and for the forwards kinematics calculation of the setpoint (initially set in respect to the coordinate frame of the augmented reality tag) transforming it into the coordinate frame of the UAV. This vector was then parsed into the component *X*, *Y*, and *Z* error (the specific measurement of meters between the desired and actual position of the UAV). Figure 18 shows the transformation process and the relationship between the tag's frame of reference, the UAV's frame of reference, and the test setpoint that we defined.

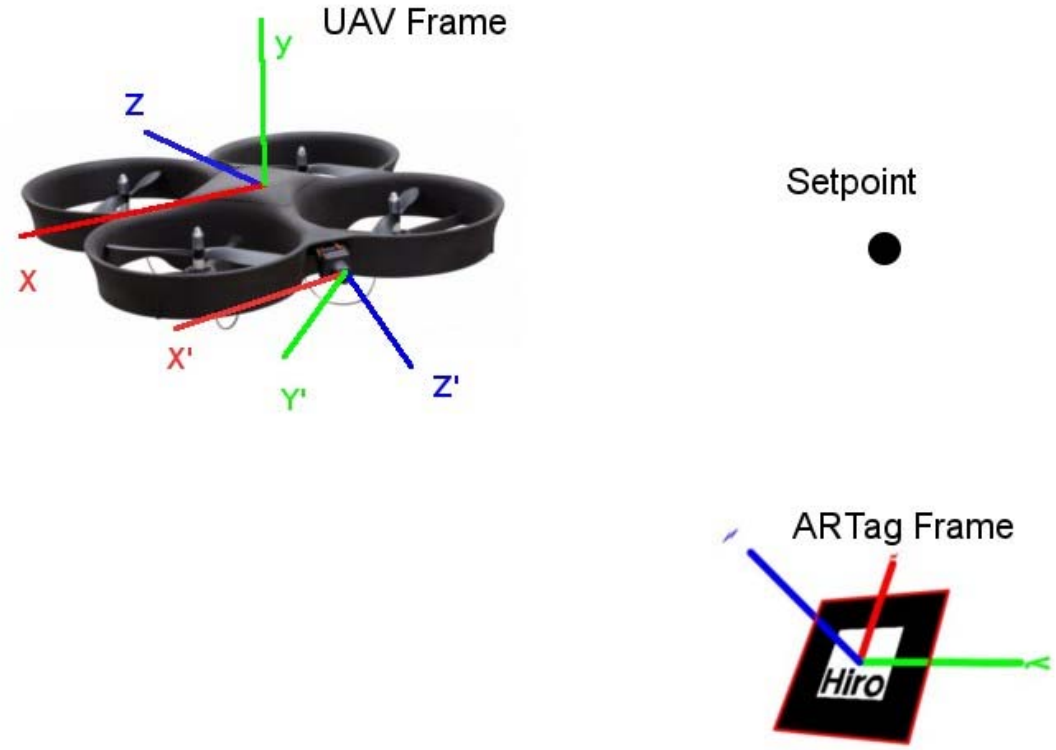

FIGURE 18 UAV TO SETPOINT FRAME TRANSFORMATIONS

Finally, in an effort to showcase the functionality of both our localization and MikroKopter control interface simultaneously, we implemented a very simple position-hold control loop. We used our previously-mentioned transformation code to calculate the error between actual UAV position and desired position, and passed these error values into a PI (proportional, integral) feedback control loop. Error in the *X* and *Z*-coordinates of the UAV were handled by setting the roll and pitch, respectively, of the UAV. For example, if the target setpoint were in front of the UAV (a negative *Z* value) and to the right (a positive *X* value), the transformation system would send a positive value to the UAV's external control pitch field and a negative value to its roll field, causing it to pitch forwards and roll right. The overall thrust provided to the system was a function of absolute magnitude of the error – the greater the error, the larger a "gas" value generate. If the *Y*-error specified the UAV was above the target location,

the gas was reduced from the amount of thrust required to hover, allowing the quadrotor to descend. If the *Y*-error indicated the UAV was below the target point, gas was added to the hover thrust to raise the UAV.

A number of situations were not addressed in our simple framework implementation of the control loop. One of the issues occurred when *uav_artag* momentarily lost sight of the tag. We implemented a solution to this problem in which the UAV would revert to the "hover" thrust and zero yaw, pitch, roll orientation when no tags were visible. Another issue left un-addressed was that of yaw control of the quadrotor. The system clearly is capable of moving in any direction horizontal to the ground plane without changing yaw (*y*-axis in the UAV frame), but for our limited testing purposes no yaw control was implemented. However, it is worth noting that in a real-world implementation, control over yaw would be necessary in order to keep the augmented reality tag in the viewing angle of the camera at all times.

uav_msgs

Unlike the other nodes in the UAV system, this node contains no actual C++ code or executables. The *uav_msgs* node provides the message definitions used in the UAV structure. Without this node, the other packages would have to contain dependencies on one another, which could potentially have caused circular dependencies if two nodes were required to communicate. Now, all quadrotor packages only depend on one standardized package to provide all of the necessary messages.

In future projects, this package will see a large amount of improvement. Any new UAV node will contribute msg files to *uav_msgs*. One such example is the *uav_command* node that had to add new high-level messages that were not implemented during our project.

3.2 ENABLE UAV LOCALIZATION

SCOPE

A number of potential real-world quadrotor applications require relative localization between a UAV and ground-based system. For example, the execution of a safe, reliable landing on the back of a potentially moving unmanned ground vehicle (UGV) requires the knowledge of the UAV's position relative to the ground vehicle in real-time with a high degree of precision. The GPS systems built into each vehicle provide an excellent method of tracking one another at long ranges. However, the resolution of the GPS modules possesses a level of error in shorter ranges that is compounded in relative position calculations.

The UAV's vision system can be employed to facilitate a more precise localization. We decided to use the vision data to control the quadrotor's relative position to the ground platform. Accurate knowledge of its location allows a UAV to accomplish a number of tasks including, but not limited to, landing. Any vision system that we developed could also be employed in a number of different future projects.

3.2.1 DESIGN SPECIFICATIONS

This project included two well-defined components; the UAV adapter (the integration of MikroKopter hardware with ROS), and system localization (the modification and encapsulation of vision processing libraries in ROS). The constraints and specifications developed in the initial phases of the project for developing this localization scheme were separated into those relating to the UAV, those relating to the ground-station testing computer containing the ROS server, and those relating to the implementation and performance of the localization system. This section presents those specifications developed in the initial planning phase of the project.

UAV SPECIFICATIONS

The method chosen for localization must easily integrate with the CyberQuad UAV platform. As such, any additional hardware required must be light enough to fit the maximum payload (500 grams) and weight distribution constraints specified for our device. Additionally, it must be able to either interface with the MikroKopter hardware boards and firmware, or operate completely independently, sending information directly to the ground station. In either case, the system could not interfere with the normal flight operations of the system.

If a camera (visual) system was used, these constraints are thus made more specific. Specifically, if a camera other than the model in the current CyberQuad package was necessary, the new system would have to integrate with the existing transmitter and camera angle-control system, or would have to be an entirely separate system.

GROUND STATION SPECIFICATIONS

While the ground station does not have weight and size requirements as specific as the UAV, there are several considerations to be made if the ground station is to remain mobile. First of all, any device used cannot exceed the dimensions of the platform. Additionally, the method for localization should not interfere with the operation of the ground station or the flight of the UAV. As such, the system should include minimal protrusions which might be hazardous to UAV flight operations. Any hardware that the ground station employs must be compatible with a Linux-based PC with standard hardware. However, in terms of this project, the main hardware limitation is that the localization device must be securely attached to the ground station.

Because the ground station must run Linux with ROS, the software developed for the localization method must be compatible with the provided interfaces. Specifically, all programs must be written in a language which can send and receive messages using the ROS constructs (currently limiting us to either Python or C++). Also, these programs must operate in real-time, and provide low-latency, accurate, and precise information about the current state of the

system. These systems must also account for connection problems, gracefully handling error conditions without damaging hardware.

LOCALIZATION SPECIFICATIONS

With a vision based system, the cameras and capture systems would need to provide a detailed view of the environment. They must provide a wide field of view, providing for a large coverage area of the ground platform, as well as providing a high-quality image. For the system to function in real world environments, the images must be returned with extremely low latency and must automatically adjust for environmental changes in lighting through adjustments in the brightness and contrast levels of the output image.

Assuming the Augmented Reality Tag system is used, the libraries used, and software developed, must be able to distinguish the specified tag from the noise of the environment. From this, the software must be able to provide position coordinates and orientation information relative to the camera's view of the tag. The software must also be able to handle views of the tag at extreme angles. Finally, it must compensate for problems with sporadic target loss.

In general, the solution for localization should provide a level of accuracy higher that what can be obtained using traditional methods, including GPS or IGS. This includes superior close-range localization, various environment support, and superior update rates.

3.2.2 DESIGN DECISIONS

INITIAL DESIGN

To properly determine its three-dimensional location and orientation with respect to a landing platform, the initial UAV design used an entirely camera-based system that tracked a specially-designed target. The image processing would run in a single ROS node, which would

then post the UAV's position/orientation information to a standard ROS transform construct to be read by the general UAV controller node. This controller was intended to serve as the governing controller for all future UAV applications. It was designed to receive all relevant UAV sensor data and make critical decisions based on this input.

FINAL DESIGN

Several augmented reality tag libraries were considered for this project: ARTag, ARToolKitPlus, Studierstrube Tracker, and ARToolKit. The key factors in our decision regarding these libraries were: product availability, tag-tracking features, camera-interface features, available APIs, and Linux compatibility. The chosen library would optimally be open source, be able to track multiple tags, and be compatible with C++ and Ubuntu Linux.

TABLE 7: FEATURE COMPARISON OF A. R. TAG TRACKING LIBRARIES

ARToolKit	• Open Source, Widely Used / Developed • Can track multiple tags • Written in C • Compatible with Linux, Windows, Mac OS • Built-in 3D Overlay Feature
ARTag	• Closed Source, No longer available • Can track multiple tags • Compatible with Linux, Windows, Mac OS • Built-in 3D Overlay Features
ARToolKitPlus	• Open Source, No longer maintained (since June 2006) • Can track up to 4096 tags • Compatible with Linux • Written in C++, class-based API • Supposedly faster than ARToolKit, with better thresholding and pose estimation
Studierstrube Tracker	• Closed Source, Not currently available (still in development) • Can track up to 4096 tags • No built-in video capture support • Support for Windows (XP, CE, Mobile), Linux, Mac OS, iPhone, Symbian • Developed as an improved successor to ARToolKitPlus

Based on the descriptions of the features provided by these four libraries, the clear choice was to use Studierstrube Tracker, mainly because it seemed to be the newest and most

actively-maintained project with the most features and support. As a successor to ARToolKitPlus, it claimed to include all the same functionality, but with improved performance. It provided the most features, the best tracking ability (based on the sample videos), and the most diverse platform compatibility. However, we were unable to procure a license to use this product.

Then, the next obvious choice would be ARToolKitPlus, since it was available, compatible with our system, provided a C++ class-based API, and was described as an improvement over ARToolKit. However, it did not provide an integrated solution for capturing frames from a video source like ARToolKit did. In addition, it did not provide a built-in feature for 3D overlays that provided useful testing information. Lastly, according to the change-logs, the last active development of ARToolKit was more recent than ARToolKitPlus.

Despite the improvements ARToolKitPlus describes, the decision was made to develop with ARToolKit. This library seemed to have more active projects than the other alternatives. By using a widely-used library, we assumed that there would be more development information and documentation available. Also, ARToolKit was still officially an active development project. ARTag was not considered because it has not been in development for several years and the source files are no longer available.

3.2.3 DEVELOPMENT

REQUIRED HARDWARE

For testing purposes in parallel to quadrotor development without employing the actual quadrotor hardware, we researched and procured several webcams for ARToolKit testing using the most widely-supported hardware available. In future projects, these webcams could also eventually be used as additional tag-tracking cameras on the ground-station. Additionally, we obtained several video capture interfaces to allow the tag-tracking software to make use of the

video from the CyberQuad sent over the wireless receiver. These webcams represent only an "optimal-case" video source because the CyberQuad would need a better standard camera available to accomplish these same results.

After our research, we obtained two webcams that we thought would be most optimal for this application: a Logitech QuickCam Pro 9000, and a Creative Live! Optia AF webcam. These two webcams were chosen because they provided a high-resolution, high-frame rate video output, auto-focus (allowing for close and far range tag tracking), and Linux compatibility.

Several standard video-quality markers were printed for use in side-by-side testing of the cameras using the Linux capture program "luvcview". Image captures were taken from the two cameras at various distances from the markers and the image quality was compared. Additionally, observations were made about the latency and frame-rate of the video image.

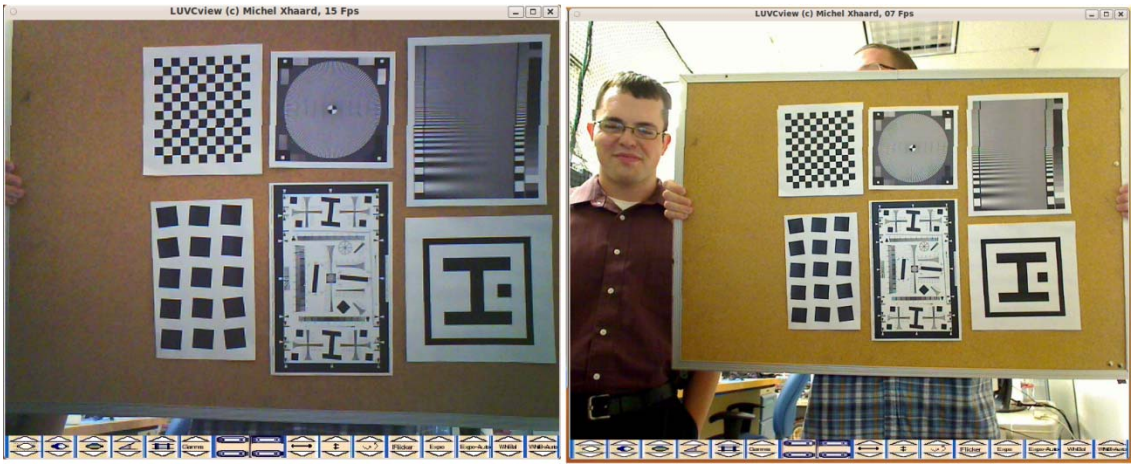

FIGURE 19: EXAMPLE SCREEN-SHOT: CREATIVE CAMERA (LEFT), LOGITECH CAMERA (RIGHT)

From these tests, we determined that the Logitech camera was the better of the two cameras. It provided a sharper image, more accurate colors, a good white balance, and a wider field of view. While the Creative webcam could focus more closely (2 inches vs. 12 inches), both were sufficient for our purposes. Additionally, this test revealed information about the cameras' performance on various resolution settings. The highest resolutions on each camera

(1600x1200) only allowed for 15fps video, versus 30fps with the standard 640x480 resolution. The higher resolution video seemed to have about 0.25 second of latency, whereas the standard resolution produced a higher latency of about 1 second.

To capture the video transmitted from the UAV, a 5.8 GHz “Nano 5.8” wireless receiver was obtained from Iftron Technologies, as well as a 4-port composite PCI video interface by Hauppauge and a USB “Video Live 2” interface by Hauppauge. A significant amount of time was spent trying to obtain and install the proper drivers for these devices so the actual video camera from the UAV could be used in testing. However, we were unable to configure the capture cards with the systems available and we decided to continue testing using only the webcams.

ARTOOLKIT INSTALLATION & CONFIGURATION

The ARToolKit Augmented Reality Tag tracking suite was designed to overlay OpenGL objects over tags shown in a video feed. ARToolKit provides functions that will return the position and orientation of the tag in a 3x4 matrix, both with respect to the tag and to the camera using a built-in transform function. Additionally, this software provides a means to calibrate for camera distortion and depth of field.

This program requires the Video4Linux and GStreamer packages be installed on the system. Video4Linux provides an abstraction of a video source (such as a webcam), and GStreamer provides a pipeline interface for manipulating video streams in Linux. According to the documentation, Video4Linux can be used alone, or in conjunction with GStreamer to connect the video input with ARToolKit.

While it may work "out of the box" on older systems, the example program binaries in the "bin" folder with default parameters did not immediately work on our system. These example programs were designed to perform simple tests, such as opening the video display and overlaying a 3-Dimensional box over an example tag in the frame. ARToolKit was originally compiled for use with Video4Linux or with a joint Video4Linux-GStreamer system, but in the

end, we were only able to get it to work with the joint Video4Linux-Gstreamer option.

Initially, we attempted to make the ARToolKit example files work with only Video4Linux because it is installed by default in Ubuntu. However, when we attempted to run any of the example binaries, the programs would immediately crash upon trying to open the video device. We assumed the problem was a result of the default parameters used to configure the camera, we modified these parameter settings. After numerous failed attempts, we chose to use GStreamer to bridge the connection between ARToolKit and the Video4Linux abstraction.

Getting GStreamer to route the video to ARToolKit in the correct format was also very difficult. Using the GStreamer utility called "gst-launch-0.10", we were able to test different pipelines and export the end result to a window on the screen. We eventually discovered a pipeline that showed the image from the webcam on the screen to verify that GStreamer could indeed read from the webcam through the Video4Linux source.

Next, we entered this pipeline into the ARToolKit example projects as the stream parameters. This, however, did not work and program crashed on launch for resolutions greater than 400x320. With this pipeline, the example program "simpleTest" opened properly and could track the example tag (the center tag from `Figure 5: Sample A. R. Tag Patterns`). This was sufficient for some preliminary testing, but the system required improvement to support the full resolution of the camera. By changing some undocumented parameters that set the Video4Linux width and height before resizing by the GStreamer pipeline, we were able to open the video source at the full resolution and track the tag.

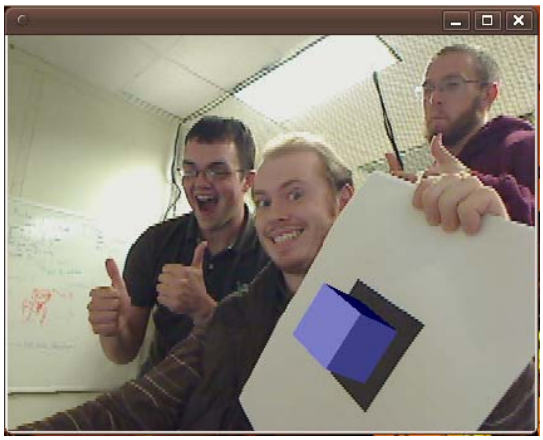

FIGURE 20: FIRST SUCCESSFUL TEST

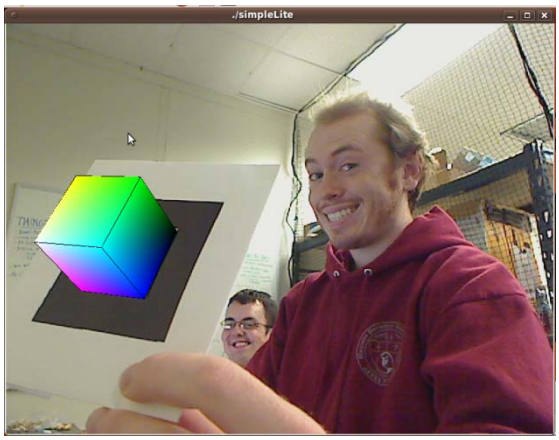

FIGURE 21: FIRST HIGH-RESOLUTION TEST

After the full resolution was obtained from the camera, we ran the ARToolKit camera distortion calibration program with the camera. This required a special grid of dots and a series of snapshots of this grid from various angles. The user then manually selected the center of each dots. By using this calibration file, ARToolKit was able to provide more accurate localization information.

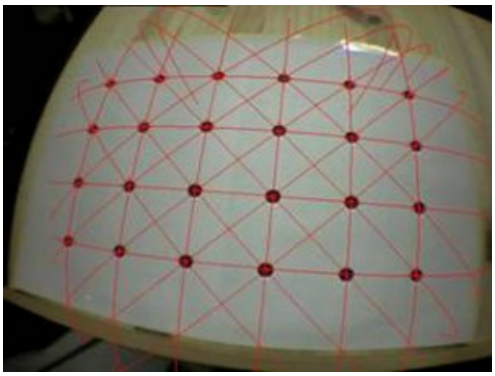

FIGURE 22: EXAMPLE ARTOOLKIT CALIBRATION RESULT

C++ AND ROS INTEGRATION

To enable ARToolKit to be used with ROS, we needed to compile the libraries alongside the executables in a ROS node. Additionally, this node had to encapsulate all of the functionality of one of the ARToolKit example programs in C++. This ROS node was called *uav_artag*, and in the end, was able to track a tag and publish both a ROS transform as well as a ROS topic

containing the transformation information.

For the first step in developing this node, we moved the example ARToolKit program "simpleLite.c" into the ROS node source directory and configured it to compile alongside the empty ROS node. This required conversion from the original standard Makefile in C into the hybrid cmake/ROS Makefile format. We had to ensure that the libraries linked to ARToolKit's installation directory. After simpleLite.c was compiled successfully in the new location using the ROS Makefile format, we began adapting the program to use standard C++ structures.

Problems were encountered upon switching from ARToolKit's original *gcc* C compiler to the *g++* C++ compiler used by ROS. The differences in how the two compilers handled memory caused ARToolKit to crash with a segmentation fault significantly more often, both during initialization and at some points while running. Many of these problems were traced to ARToolKit functions that did not fully specify any return values or array indexing and memory access errors. Once we created and applied patches to the ARToolKit libraries, the program crashed much less frequently; however, unresolved problems in the ARToolKit libraries still exist. These changes and problems were extensively documented on the Lincoln Lab wiki page.

To start the conversion of ARToolKit's C code into C++ style, we modified the ARToolKit example program to create an "ARTag" object. We also made the previously-global functions and data public or private as needed. Additionally, the appropriate initialization functions were created for the variables, including the new ROS structures. This example program became the entirety of *uav_artag*.

After the basic conversion was complete, we encountered a problem regarding OpenGL and GLUT, the 3D rendering system that ARToolKit uses to draw to the screen and perform transform translations. Because OpenGL is written in C and is not inherently object-oriented, only one instance can be used in any given process. It maintains configuration information internally and cannot be used for multiple objects. We changed the code to store a global pointer to the C++ object upon instantiation and created global wrapper functions for the C++ methods.

To allow multiple ROS ARToolKit nodes to exist and communicate, we used standard ROS parameters from the Parameter Server as a method of configuring the GStreamer, tag, and camera settings. These parameters could be set in a ROS Launch File, or, if left unspecified, set to the defaults defined in the C++ class.

The next step in the development of the localization scheme was to address the conversion between ARToolKit output data and ROS transforms. The transformation matrix returned by ARToolKit, containing the rotation and orientation of the tag, was returned as a 3x4 transformation matrix. ROS transforms, however, use a different format, known as "Quaternion", to store the rotation information. Thus, the transformation matrix was separated into the location and rotation elements, and these elements were used with ROS conversion functions to create the standard ROS transform objects. These transforms are different than standard topics and are always available to every node. However, because a transform is not included in a ROS bag file, we converted this transform into a standard ROS topic containing the same information. These transform messages were verified using the ROS built-in transform visualization application, *rviz*. Figure 23 shows an example of ARToolKit transforms being converted into ROS transforms and their visualization in *rviz*.

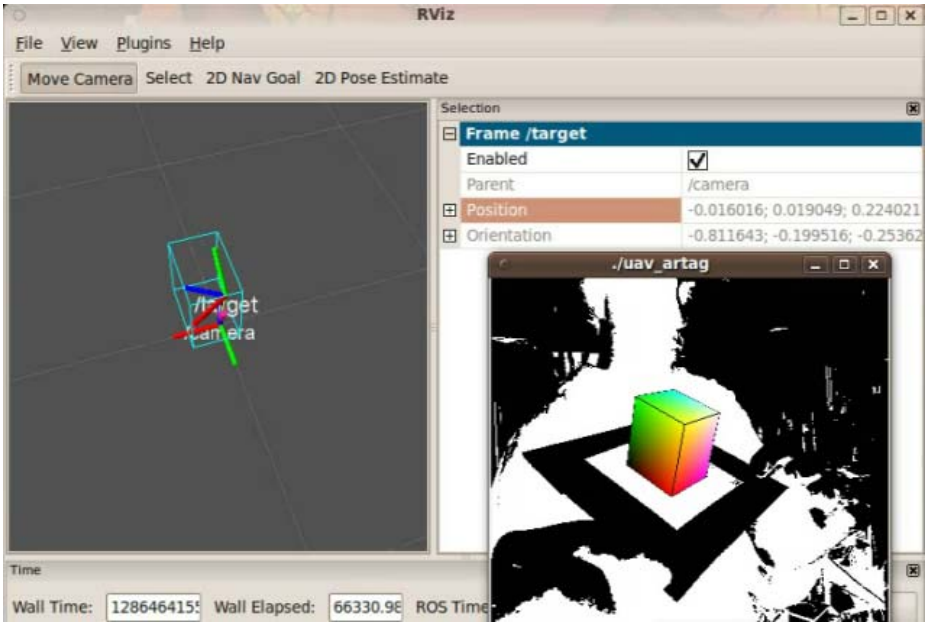

FIGURE 23: RVIZ VISUALIZATION

ARTOOLKIT TEST PROCEDURE

Several tests were performed to determine the characteristics of the tracking system. Tests were performed to quantify the scaling factors in the X, Y, and Z directions, maximum range, maximum angles at different ranges, and general variability of the measurements. These scaling factors were required to find the actual coordinates because ARToolKit does not provide the ability to configure for real-world coordinates accurately. Also, there is no guarantee that the dimensions (especially X and Y versus Z) will be scaled equally, due to variable camera focal length.

TESTING FIXTURE

Before any tests could be performed, we created a testing fixture to allow for precise positions and angles of the camera and target tag positioning. To establish a reliable testing fixture, we employed two tripods, each with the ability to easily adjust the angle of the head. The camera and tag were fixed to these tripod heads using tape.

The camera was calibrated by using the target tag on the tripod. First, *uav_artag* was modified to print out the X, Y, and Z perceived coordinates and a timestamp every time a message was sent for the duration of these tests. The end result of "calibrating the camera" on the tripod was such that the act of moving the target away from the camera along a straight line on the floor did not cause the perceived X and Y position values to change. Assuming the tag originally started at the X-Y origin (center), the lack of X-Y variation means that the camera is perfectly level with the floor. We ran *uav_artag* and adjusted the parameters on both tripods until the tag was as near the X-Y origin as possible.

POSITION SCALING FACTORS AND VARIABILITY

To determine the scaling factors in each dimension, we performed a series of tests that compared the perceived values from ARToolKit with the physically measured values. During this testing phase, we tested each dimension individually while the two other dimensions were held as constant as possible. Additionally, the tag orientation remained as fixed as possible and always faced in a plane parallel to the camera. After moving the target tripod, the new distance offset was measured using a measuring tape, and then *uav_artag* was started, printing coordinates to the screen. For each offset, samples were reported to the screen and one second worth of data was randomly selected, using the corresponding timestamps.

Specifically for the Z-direction measurements, the X and Y coordinates were held as constant as possible, with the target tag held as close to the center of the frame as possible while the target moved away from the camera until it was no longer detected. For the X-direction test, the Y and Z coordinates remained fixed while the target tripod was moved left and right. A similar test was performed for the Y-direction in with the X and Z coordinates were fixed and the target tripod moved up and down. However, because it was unknown if there was a relationship between the Z value and the X or Y value, the same tests were performed again for the X and Y dimensions, using different Z distances.

By assuming that the other two dimensions were fixed during measurement, we could plot the perceived offsets versus the actual measured offsets to determine the linear relationship between the two and convert the ARToolKit units into actual units. Additionally, by collecting one second's worth of samples, we received information about the sample rate, as well as the ability to derive the approximate measurement error using the model.

ANGLE MEASUREMENT ACCURACY AND VARIABILITY

Our next test helped us to obtain a general sense of the accuracy and variability of the angles being measured by ARToolKit. During this test, the target tag, set at the same height as the camera, was moved to various distances away from the camera, and ten samples were taken from ROS of the *roll, pitch,* and *yaw* angles. For each distance, samples were taken on the left and right extremes of the frame, as well as in the center. We assumed that the vertical axis showed similar results if the tag was instead moved up and down. We determined the accuracy and variability of ARToolKit using actual measured angles of the tag and these samples taken from ROS.

MAXIMUM ANGLES AND RANGE APPROXIMATION

Our next test was to gain a general understanding of the maximum range of the ARToolKit system. The question of range depended on the camera resolution, the tag size, the position in the frame, the lighting conditions, and the maximum required recognition angle. As such, the test was performed to provide an approximate answer for the specific setup utilized during this testing phase.

During this test, the target tripod, at the same height as the camera, was moved to different distances away from the camera along the far left edge of the image frame. Next, at each distance, we varied the yaw of the tag by rotating the tag clockwise until the tag was no

longer consistently or accurately detected. Similarly, at each distance, the yaw of the tag was rotated in the counter-clockwise direction. This first test would determine the worst case angle for that distance, and the second determined the best case.

This measurement was performed several times, moving back until the maximum detection angle range was very low, detecting the tag only when flat forward to the camera's plane of view. This test shows approximately the ranges of camera angles available at different distances, assuming the target is aligned vertically in the center of the frame.

MESSAGE UPDATE RATE

To test the average rate of messages being sent by ARToolKit, we ran statistics on the previously collected data. Since each sample set for distance measurements was taken over a one second period, the number of samples in those time intervals readily available. We created a frequency histogram for each sample that shows the approximate rate distributions for this particular PC and camera.

3.3 DOCUMENTATION

This project also produced information which will allow future projects to easily extend our work. As such, each step of the procedure has been documented clearly in the Chapter 3 of this report, describing any problems that were encountered and outlining reasons behind all major project decisions. The report also includes general information about how the project progressed.

Additionally, we produced a Wiki page which provides detailed information regarding the specific configuration of the system, including setup and testing procedures. It also includes reference information about the UAV hardware and software. The software documentation

describes higher-level functionality and how to use the developed software API. This page should be the primary resource for those seeking to investigate similar projects.

All code that is produced by this project is extensively documented in a readable, understandable fashion. In keeping with MIT Lincoln Laboratory's existing software, we emulated their methods of documentation for ROS nodes in which non-default or non-intuitive ROS functions are described. The documentation of the quadrotor's adapter software involves much more detail than the Laboratory's existing code on the grounds that this project will be picked up by an entirely new team with no knowledge of the adapter's API. Additionally, the code is written in a modular and generic way, so pieces of it can be applied to other projects without significant modification. It will be kept in source control for future Lincoln Laboratory development. The types of documentation for the CyberQuad include:

- Software documentation
- System hardware documentation
- Relevant software installation procedures
- Instructions for the use of completed deliverables
- Lists of unimplemented functionality
- Recommendations for future development

Our project aimed to provide MIT Lincoln Labs with a UAV system that will function as a step in the direction of real-world quadrotor applications. Our goal was to simplify future development, as well as to demonstrate the potential of the CyberQuad UAV to the Laboratory's robotics division. The development of a system by which a UAV can be controlled via computer, in particular, is great evidence that a number of proposed real world autonomous quadrotor applications are viable. . With the tools we have provided, there is little doubt that the CyberQuad will be a vital component of Lincoln Laboratory's future UAV development.

4.0 RESULTS AND ANALYSIS

Our project aimed to provide Lincoln Laboratory with a basis for further development of the CyberQuad platform. As such, we tested our designs and implementations to determine their feasibility in future applications. Each element of the project - the interface, the localization scheme, and the documentation - provided useful information for use by future developers. This chapter presents all measureable data collected over the course of the project, as well as some analysis, to demonstrate the effectiveness of the features implemented during this project and to provide documentation for future endeavors.

4.1 PC CONTROL INTERFACE

The first major section of this project was the development of the UAV adapter system that allowed for PC communication to and control of the CyberQuad. All testing performed in this section primarily involved analysis of this communication to and from the quadrotor. We measured the connection strength, speed, and robustness. This section also involves an evaluation of the performance of the various nodes created over the course of the project.

4.1.1 *UAV_HEALTH_MONITOR*

The purpose of this ROS node was to provide future developers with a tool which provides a metric for how well the computer is communicating with the CyberQuad hardware. This would provide them with a general sense of which maneuvers are possible (complex versus simple actions) given a certain level of degraded control and communication. If this information was not taken into consideration, poor link conditions could potentially cause too many missed commands and a poor reaction time, potentially leading to a disastrous result.

Testing of this node allowed us to gain an understanding and a reasonable measurement of the quality of the serial link between the ROS master PC and the CyberQuad under various conditions. The *uav_health_monitor* served to calculate both the latency of the connection, and

to keep track of the number of dropped messages. This data could then be used to determine if the quadrotor would be able to operate consistently in real-world situations.

To conduct testing of this node, the latency was logged in three separate tests. The first test involved running the *uav_health_monitor*, *uav_command*, and *uav_adapter* nodes. The *uav_command* was run in this case because it subscribes to the *uav_health_monitor*'s output messages, displaying the latency and link health to screen as well as logging the data to disk. Using this data, graphs and tables were generated, as presented in this section. Figure 24 shows the results of the latency test when running the nodes listed above.

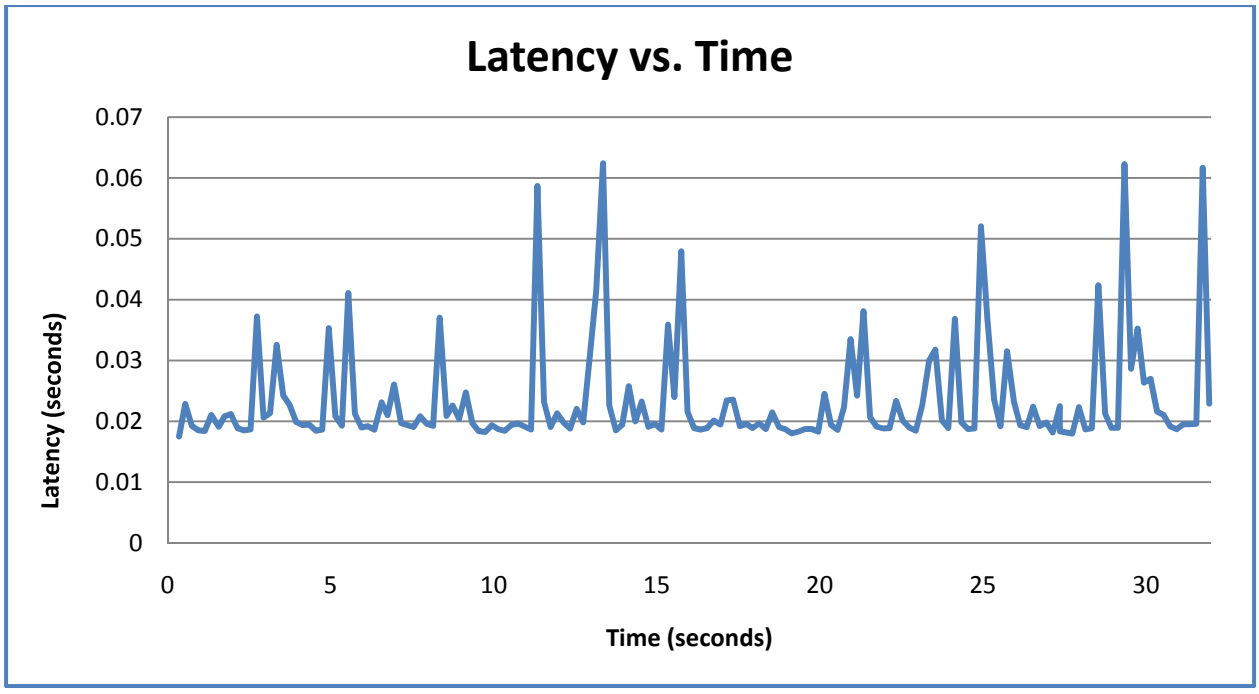

FIGURE 24: LATENCY IN HEALTH MONITOR TEST

In this test, the latency was consistently above 0.018 seconds, spiking as high as 0.062 seconds at points in the test. More specifically, the average latency over 30 seconds was 0.023 seconds with a standard deviation of 0.0087. We determined this latency to be low enough for

most applications of the quadrotor. The low deviation in the connection also demonstrated sufficient reliability of the system for normal use.

The previous test provides a good sense of link latency of simple commands without a heavy load over the serial port. However the results were not necessarily consistent with the operation of the full system working together. To properly test the link during heavier and more realistic loading of the system, we ran a second test that employed the *uav_health_monitor*, *uav_translator*, *uav_adapter*, *uav_command*, *joystick*, and *uav_teleop*. The operation of all of the nodes simultaneously provided the best possible representation of a fully-operational quadrotor system. Figure 25 shows the graph of the system's latency over 30 seconds with all of the UAV's features operational, including external control.

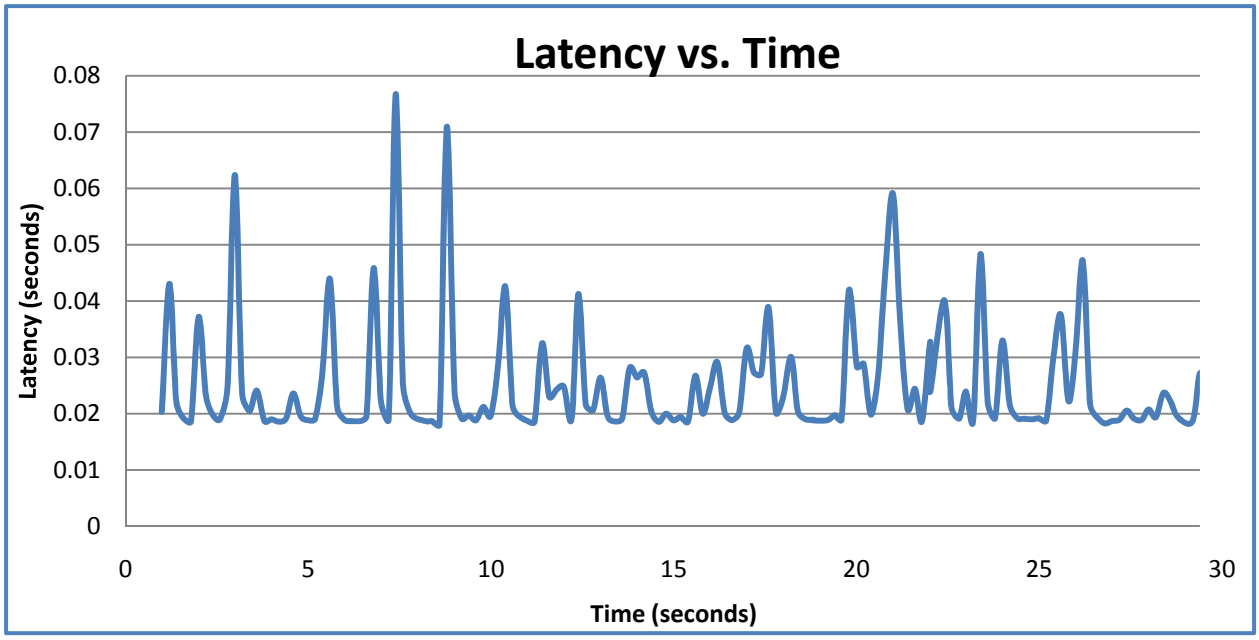

FIGURE 25: FULLY LOADED LATENCY TEST

In the second test, the latency proved to be only slightly less stable, and nearly just as low as in the lower-operation test. The average latency was 0.025 seconds, while the standard deviation was 0.0101. Based on this data, we determined that the serial link, and the

functionality that we created to manage its operation, work well enough for this quadrotor to react appropriately in real-world applications.

The above tests were completed over an interval of 30 seconds to more clearly, visually demonstrate the operation. These second of these two tests, however, was repeated over 1000 seconds to analyze the performance over time – particularly, whether the link health would degrade with time. The histogram shown in Figure 26 below represents the results of the test over the extended time period. The majority of the latency results remained in the area of 0.025 seconds or less, even over the long time period. This suggests that the quadrotor command response would be somewhat consistent the majority of the time.

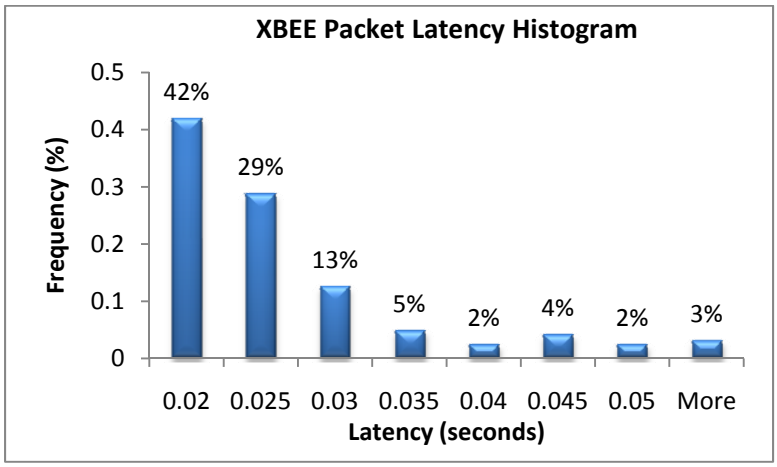

FIGURE 26: LATENCY OF FULLY-LOADED SYSTEM

Once latency was evaluated, the next important step was to evaluate the overall stability of the connection. The *uav_health_monitor*'s functionality to calculate the number of packets dropped served as the basis for this test. Two tests were performed on the link, each identical in setup to the previous two tests: the first test involved light-loading of the system, while the second involved full-loading.

In the first test, the link health remained at 100% over the 30 seconds of testing. As such, we can assume that there would be few problems with the serial connection with these few

processes running. The consistent link health persisted over the full range of the test, demonstrating that time was not a factor in the link's health.

Under full loading, a small number of messages were dropped over the course of the full range testing. In this test, the link health averaged at 98.82%. The lowest link health reached was 96%, which, based on the configuration of the sampling frequency and queue size, represents 2 dropped messages per 50 messages sent (or about 1 message every 1.7 seconds, based on the 15 Hz message send rate). Figure 27 shows the link health for a 30 second sample of the full 1000 second test. Note that this behavior, varying between 100 and about 98 percent, repeated over the course of the full test.

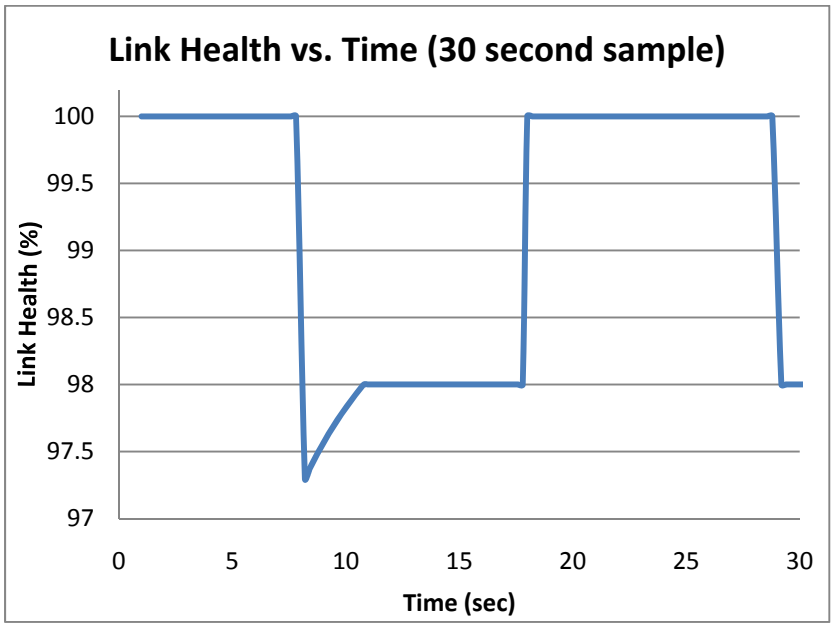

FIGURE 27: LINK HEALTH DURING FULL LOADING AT 15HZ

Later, we tested the quadrotor with different external command sending frequencies to see if the bandwidth of the serial port would be exceeded. In Figure 27, the publishing frequency of external control messages was 15 Hz. We tested the system again at frequencies of 10Hz,

30Hz, and 50Hz. At 30Hz, there was no measureable change from the 15Hz test. At 50Hz, however, we did notice a significant change in the link health.

Below, Figure 28 shows a 100 second sample from the 50Hz test. The average link health over this duration was still 97.18%, though this decrease over time. The increased frequency of the external control publisher resulted in more dropped *serial_link_test* messages. The general decline apparent in Figure 28: Link Health Under Full Loading at 50 Hz, however, did not continue after 100 seconds. The link health continued to fluctuate within the same range, never reaching lower than 88%. While we determined that this link health was still sufficient to fly the UAV in a real-world environment, we needed to discover the cause of the dropped messages.

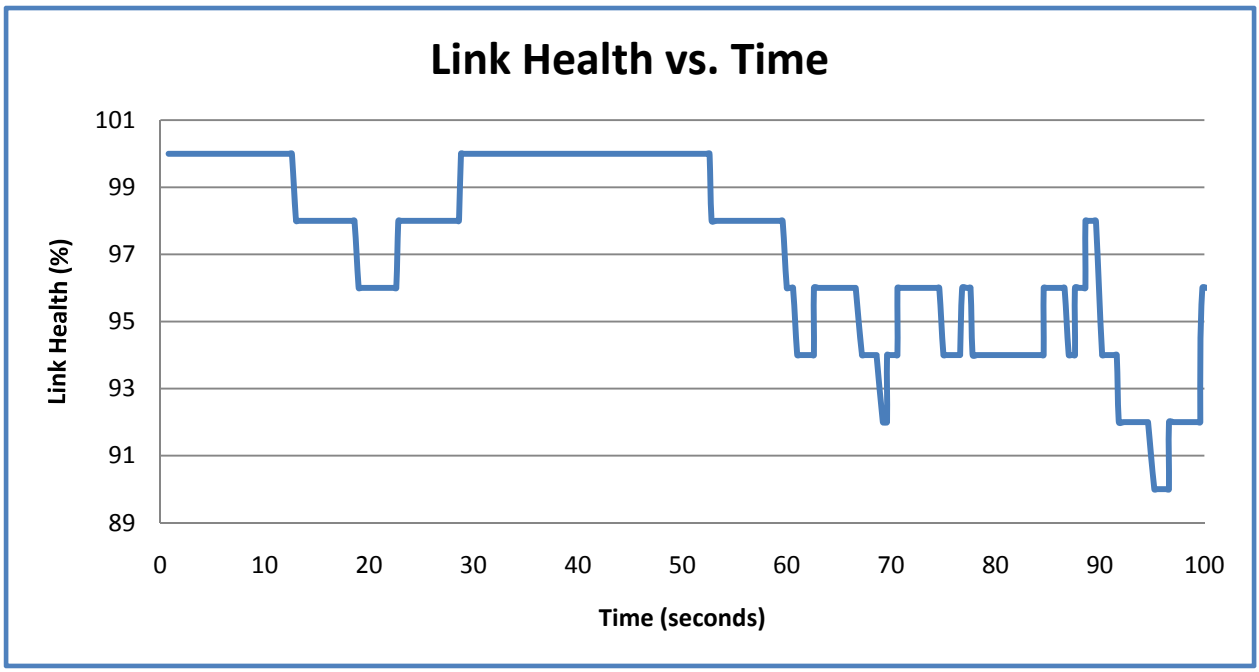

FIGURE 28: LINK HEALTH UNDER FULL LOADING AT 50 HZ

We theorized that there were three possible explanations as to why messages were dropped:

1. During this test, the large volume of messages passing through the serial port blocked the serial connection and the messages were ignored by ROS and not sent to the CyberQuad hardware.

2. The external commands required too much of the CyberQuad's processing power and it was unable to reply with the proper when an EchoPattern is received. The EchoPattern could have either been returned out of order or skipped altogether.
3. The XBEE wireless serial modem would occasionally drop messages or corrupt packets during normal operation.

We performed a new set of tests to narrow down the cause of the dropped serial link messages. This test employed a direct cable connection to CyberQuad, as opposed to the XBEE wireless modem. If no messages were dropped while using the serial cable, we could determine the cause of the imperfect connection. In this test, the UAV system was run with full loading and an external control publishing frequency of 50Hz. Figure 29 shows a 30 second sample of the latency results of this test with the MKUSB cable attached, rather than the XBEE wireless module.

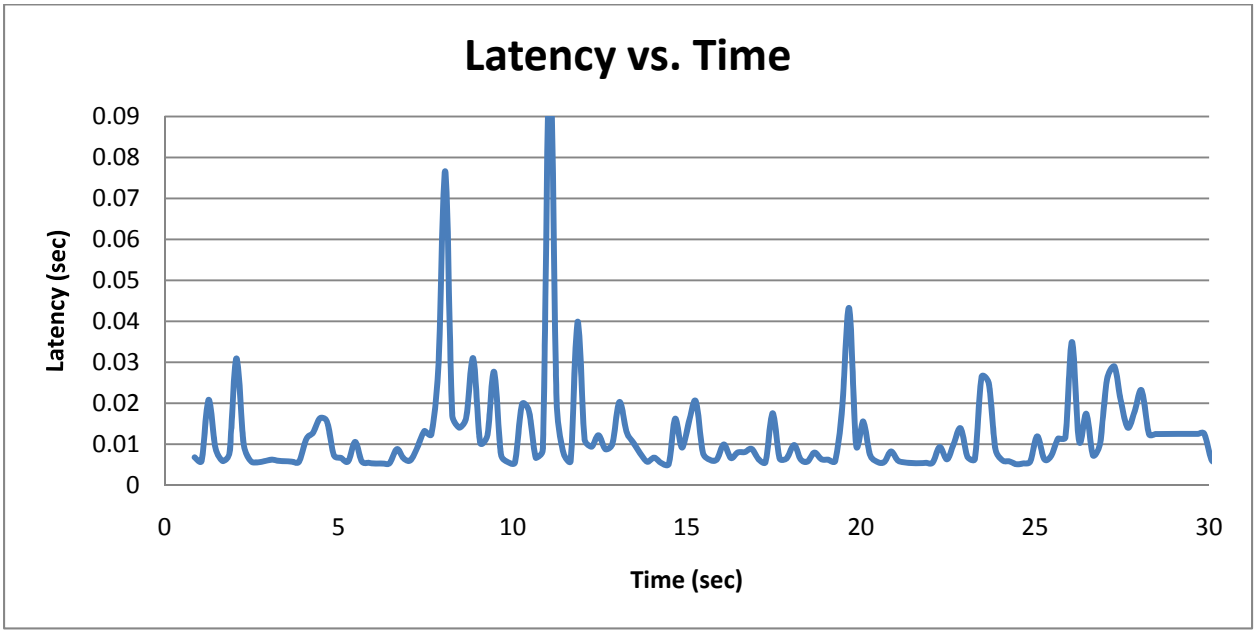

FIGURE 29: LATENCY AT FULL LOAD WITH SERIAL CABLE CONNECTION

The average latency in the test of the direct serial cable connection was 0.012 seconds with a standard deviation of 0.01 seconds, having nearly half of the latency as that obtained by the XBEE. Figure 30 shows the latency of this test over the full test. In comparison to the previous test with the wireless serial connection, the majority of the MKUSB's latency results were below 0.015 seconds, as compared to the majority being under 0.025 with the XBEE.

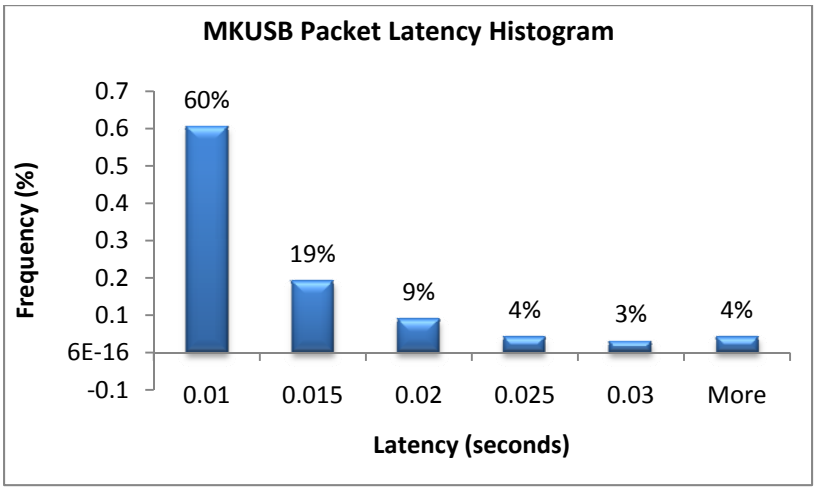

FIGURE 30: LATENCY FOR FULL LOADING -WIRED CONNECTION

Additionally, in the serial cable connection test, the number of packets dropped over the full 1000 seconds of testing was also recorded. The system had 100% link health throughout the test, proving that dropped messages recorded in previous tests were a result of the wireless serial connection. Even though the direct cable is superior, the quadrotor cannot operate while attached to a cable in a real-world scenario. A wireless system is mandatory for most applications, but these tests demonstrate that it is an imperfect solution. Future applications must either factor this potentially flawed link into account when planning aggressive or command-intensive maneuvers or devise a new communication scheme to be more reliable.

While the *uav_health_monitor* provided useful information regarding the status of the serial connection, this information was entirely based on the *serial_link_test* command sent to

and received by the CyberQuad hardware. This command was designed specifically for the purpose to which we applied it. Testing only this command, however, does not inform the system as to whether or not an important message (such as navigation waypoint planning or external control) is dropped. It can only determine if a *serial_link_test* message is dropped. As such, adding future functionality for tracking important messages must be implemented.

4.1.2 UAV_TELEOP

The *uav_teleop*'s ability to send external control messages to the CyberQuad makes it one of the more important features of the quadrotor's control system. When completed, we tested the operation of this node on the CyberQuad. During testing, we realized a number of important features that needed further exploration.

The first major consideration in the operation of the *uav_teleop* was the reaction time of the quadrotor. In the very first trial of the fully-operational system, when the joystick was depressed, the UAV experienced a delay before reacting. The amount of delay time varied from test to test, but was always noticeable to the tester. Having a reaction time this slow would likely mean the quadrotor would have problems operating with high-speed closed control loop, as would be necessary in a real-world environment.

As a result, a test was performed with a smaller load on the ROS computer, assuming the delay was an artifact of slow computer hardware, or inefficient programs. Before beginning the test, ROS was restarted, all non-required processes were closed, and the UAV system was controlled through the command line, rather than the eclipse development environment. The resulting quadrotor performance appeared to be improved from the previous trial, though a delay time was still noticeable. Though likely still not fast enough for precise control, the quadrotor could have likely been piloted remotely at higher altitudes using the perceived amount of delay.

To address the fluctuating delay time, we tested the quadrotor with a number of different update rates from the joystick node. By changing the joystick node's update rate, we were able to determine one cause of delay time in the system. One theory was that the 15Hz refresh rate that we used by default placed too much strain on the serial connection and overflowed the serial connection's bandwidth. The other theory was that a higher refresh rate would send more continuous commands to the CyberQuad to help give it more stable control and smooth movements. We tested a number of frequencies to determine which appeared to consistently produce the lowest latency and the smoothest transitions between joystick-directed movements. These observations are summarized in Table 8 below:

TABLE 8: CONTROL OBSERVATIONS, VARYING JOYSTICK UPDATE RATE

10 Hz	• Delay time no noticeably different than at 15Hz • Very crude motion with jerking and jumping from one speed setting to another
15 Hz	• Slight delay in response • Jerky movements when the control stick was moved quickly
30 Hz	• Delay time no noticeably different than at 15 Hz • Movements slightly smoother than at 15Hz
50 Hz	• Delay time no noticeably different than at 15 Hz • Smooth movements • Easier to control properly
100 Hz	• Delay time no noticeably different than at 15Hz • Smoothest movements achieved • Easy to control properly

Overall, based on the quadrotor's performance at the various frequencies, we determined that the best publishing frequency for the external control would be in the range of 50 to 100 Hz. The most optimal quadrotor flight was achieved at 100Hz. When operating many other processes in ROS or sending more commands to the CyberQuad, however, this frequency might result in a bandwidth overflow, due to the large packed data structures being sent over the serial connection, or unacceptable reductions in the operating speed of the PC. The best possible external control publishing frequency requires a tradeoff between smooth controls and link

health. The frequency should be set at the highest possible value without consistently overflowing the bandwidth – a frequency that must be both determined on a case-by-case basis, based on the PC's hardware configuration, as well as the fixed 57600 baud speed of the serial interface.

4.1.3 UAV_COMMAND

In order to demonstrate both computer control of the quadrotor and an accurate vision-based localization scheme working in conjunction, a simple algorithm was created in the *uav_command* node that takes in a user specified position and then calculates the relative difference in positions between the UAV and the user-specified "home position" in the frame of the UAV. These values can then effectively be used in error-based control in a simple control loop, allowing for autonomous position seeking and holding.

The performance of this system is very much dependant on the performance of the two main facets of this project: the external control commands, and the ARToolKit localization. The UAV position error is entirely reliant on the *uav_artag* node (with the addition of several static ROS transformations to handle the anticipated camera offset from the center of rotation of the UAV) and therefore suffers from the same restrictions that were revealed by the testing of ARToolKit. Likewise, the actual speed at which commands can be sent to the UAV by wireless serial is limited by the fixed baud rate of 57600, full-system latency, and general link health issues. Taking these problems into consideration, the decision was made not to attempt to test the system in free flight, but rather to mount the UAV in a test fixture and move the webcam above the UAV's target tag in order to simulate a complete system. Doing this, we were able to track the resulting error vectors on a screen printout and watch the physical motions of the UAV to confirm that correct position correction was occurring.

Although the restrictions on flight as a result of the testing fixture prevented extensive testing or tuning of the control loop, it was obvious from terminal output and the ROS Rviz

transform visualization tools that the correct error vector was being generated relative to the UAV's frame of reference. Likewise, from the debugging information it was apparent that the correct error compensation messages were being generated reliably. Moving a point simulating the UAV's position away from the setpoint correctly resulted in the corresponding pitch and roll compensations to correct the motion. Moving the camera below the setpoint correctly results in an increased thrust. These results indicate strongly that integration of the PC control interface and localization scheme is feasible.

However, no similar success was ever achieved in accurate UAV motion based on the error calculations. The resulting motions of the quadrotor based on the output of *uav_command* proved to be erratic. The cause of these issues remained unclear. The most likely reason for the delayed, sporadic movements was system latency. From visual observations, we noted that the majority of the time the UAV reacted in a way that was consistent with our expectation; however, these actions were often delayed by several seconds, indicating that the external control latency in conjunction with any localization latency was exceeding reasonable operating parameters. Additionally, the jerking behavior that occurred during testing may be a result of similar publishing rate issues experienced during joystick testing, which were mitigated in those tests by increased message rates. In this experiment, the output of *uav_adapter* was limited by a hardware configuration bottleneck that occurred in *uav_command* that prevented the external control message rate from exceeding 15 to 20 Hz. This prevented us from attempting the same solution discovered during the joystick testing. Many of these symptoms could have been a result of insufficient hardware resources, and future efforts to distribute the processing load of machine vision, control loop, and serial I/O among multiple machines may be worthwhile.

Another possible explanation for this delay was unconditioned sensor issues. The error of the feedback loop was completely dependent on the information provided by *uav_artag* . This data proved often to be volatile and, under certain conditions, the reported angle of the

target jump unexpectedly to radically different values for a message or two. This problem, combined with frequent dropped targets or false positive tag acquisitions in different locations (very near or very far) also resulted in unreliable system performance. These concerns strongly demonstrated the necessity for additional work in visual processing before real-world systems could be reliable.

4.2 ARTOOLKIT RESULTS

The results of the tests performed on ARToolKit and the *uav_artag* discussed in this section provide an important insight into the performance of the library, both qualitatively and quantitatively. While the testing of the library was not entirely complete due to time constraints, it provided a strong background as to the plausibility of ARToolKit as a UAV localization scheme.

4.2.1 POSITION SCALING FACTORS AND VARIABILITY

The first step in analyzing the performance of ARToolKit was to identify the scaling factors used in the library – i.e. the relationships between the output results of ARToolKit and real-world values. Based on measurements performed during tests, we determined the scaling factors along all three dimensions and the error in the measurements along each axis. By graphing the perceived distance (the output results from ARToolKit) versus the real-world, measured distance and drawing a trend line, we determined the scaling function. The figures below show the test results along three dimensions - the *z*-, *x*-, and *y*-offsets from the camera. These scaling results were used to determine the error between the actual measurements and the scaled results from ARToolKit. This data is represented below in Table 9.

We observed that distance did not seem to affect the average measurement for the horizontal and vertical axis, based on the data from the 2ft and 4ft measurements. These sets of

data were graphed together, thus adding to the number of data points used when calculating the scaling factor. The important information (the difference in number deviations) was maintained by calculating this separately for each dataset as shown in Table 9.

The approximate maximum distance for detecting the tag when directly in line with the camera was 3530mm (11.6 feet). With this tag, the minimum detection distance was approximately 106mm (0.35 feet). However, when using the maximum resolution of the camera, ARToolKit could only detect the tag up to about 215mm (0.71 feet).

Though it was less noticeable for the two short-distance measurements (2 and 4 feet), the deviations in perceived distance increased as the distance from the camera increased. This can be seen in Figure 31 below, as the sample points spread out as the distance increased. This result appeared logical, as the tag representation to ARToolKit used fewer and fewer pixels as the distance increased. This result was further demonstrated by the Standard Deviation of the error for the tests, shown in Table 9. The shorter distance tests exhibit error deviations of about 1 cm and less, whereas the error deviation for the long distance test is about 3 cm. This number was likely higher because the test included more long-range positions, with the increased distance causing increased deviation.

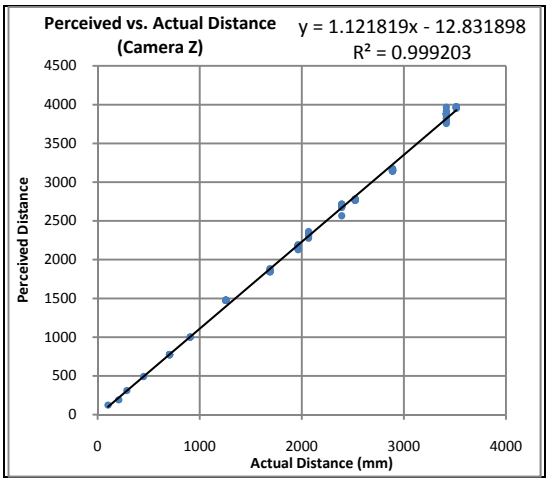

FIGURE 31: PERCEIVED VS. ACTUAL Z-OFFSET

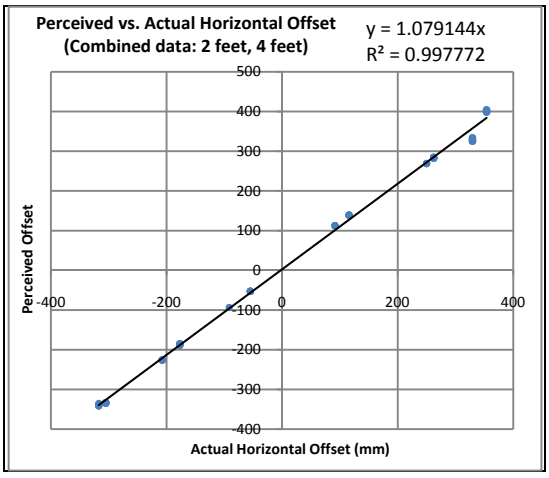

FIGURE 32: PERCEIVED VS. ACTUAL X-OFFSET

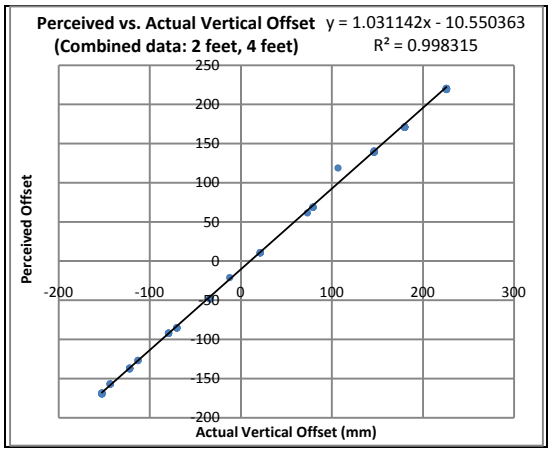

FIGURE 33: PERCEIVED VS. ACTUAL Y-OFFSET

TABLE 9: MEASURED VS. PERCEIVED X-Y-Z OFFSET ERROR

(in mm)	Z-Offset	X-Offset (2 ft)	X-Offset (4 ft)	X-Offset (combined)	Y-Offset (2 ft)	Y-Offset (4 ft)	Y-Offset (combined)
Error Standard Deviation:	32.25884	10.7061	5.58197	10.97756	7.08232555	0.951631	5.197521
Average Error:	22.87656	1.00134	-5.35594	-2.36570	1.01897E-06	-0.00725	0.480358

4.2.2 ANGLE MEASUREMENT ACCURACY AND VARIABILITY

This test sampled the yaw, pitch, and roll at three positions for each distance (far right, far left, and center of the frame). The data for all three positions was grouped and graphed together to demonstrate any correlations in the results. Particularly, we observed if there were any correlations between the position in the frame and the angles that were recorded. These graphs for the roll, pitch, and yaw deviations are shown below.

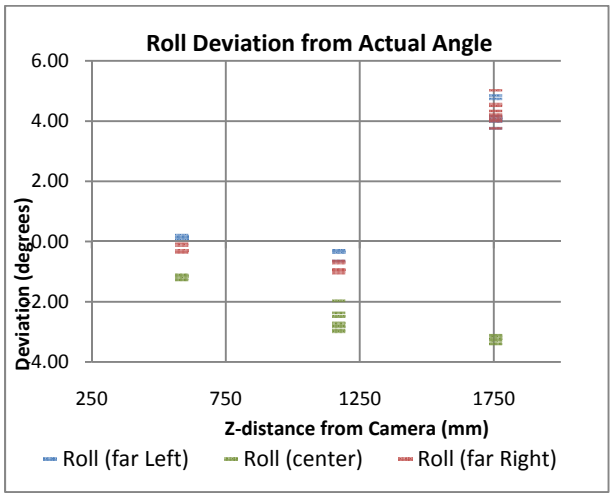

FIGURE 34: ROLL DEVIATION

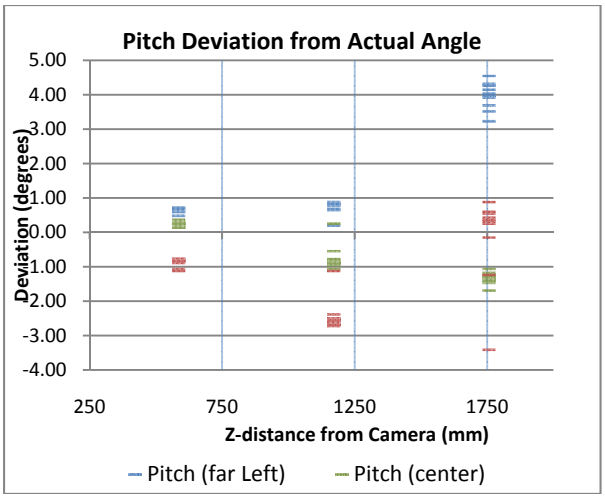

FIGURE 35: PITCH DEVIATION

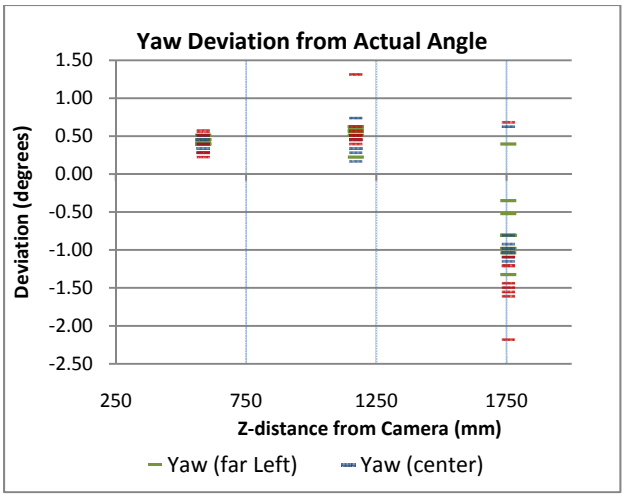

FIGURE 36: YAW DEVIATION

Based on the above graphs, it was hard to find any sort of well-defined correlation between the positions in the frame and the deviation from the actual angles. We had assumed that for the left and right extremes of the frame, there would have been a larger error from the actual angle, with this error increasing as the distance increased. The data supported this assumption, though not entirely consistently.

The graphs above, especially Figure 34 and Figure 345, clearly show that the measurements taken in the center of the frame had a smaller error than the edge measurements overall. Additionally, as the distance increased in each experiment, the angle error increased as

well. However, the error was not increasing in a consistent manner, with the data groupings for each set of samples varying between positive deviation and negative deviation between measured distances.

Looking at the data further, we drew some important conclusions based on certain trends in the data. Below, Table 10 shows the standard deviation for all sample sets taken during this test. After averaging the deviations at discrete distances, it became apparent that as the distance from the tag increased, the deviation also increased. At 6 feet from the camera, the deviation in angle was about six times greater than at 2 feet, with a deviation about 0.5 degrees within the sample set. This was consistent with the observations for sample-set coordinate deviations described previously.

TABLE 10: STANDARD DEVIATIONS OF MEASUREMENTS (ALL)

	Roll			Pitch			Yaw			Averages
	Far left	Center	Far Right	Far left	Center	Far Right	Far left	Center	Far Right	
2 feet	0.042	0.061	0.095	0.068	0.070	0.121	0.047	0.087	0.133	**0.0804**
4 feet	0.103	0.329	0.137	0.208	0.387	0.496	0.128	0.103	0.276	**0.2410**
6 feet	0.342	0.100	0.356	0.396	0.170	1.287	0.477	0.524	0.744	**0.4884**

Additionally, Table 11 below describes the deviations between the samples at all distances combined. This data describes the error one can expect between samples at different distances in different positions in the frame. Therefore, it gives a better idea of the sorts of variations one should expect throughout the detection range. Between the roll, pitch, and yaw measurements, the largest standard deviation was for the roll at 2.51 degrees. Therefore, the general error in angle, when reflected generally, was ±2.5-3 degrees of error in each direction.

TABLE 11: STANDARD DEVIATIONS OF MEASUREMENTS (COMBINED 2 FT, 4 FT, 6 FT)

	Roll			Pitch			Yaw		
	Far left	Center	Far Right	Far left	Center	Far Right	Far left	Center	Far Right
Std. Dev. (degrees)	2.08	0.90	2.35	1.60	0.70	1.24	0.64	0.67	0.97
Overall Std. Dev. (degrees)	***2.51***			**1.77**			**0.769**		

4.2.3 MAXIMUM ANGLES AND RANGE APPROXIMATION

Based on the measurements performed during these tests, we obtained an idea of the maximum tag-detection angles achievable and angle measurement error. Below, `Figure 37: Tag-Detection Angle Graphic` represents an overall summary of the test procedure. We calculated the maximum clockwise and counter-clockwise angles for tag detection in the far-left and center of the frame. The two graphs below detail the angle detection data that was collected for these two test scenarios.

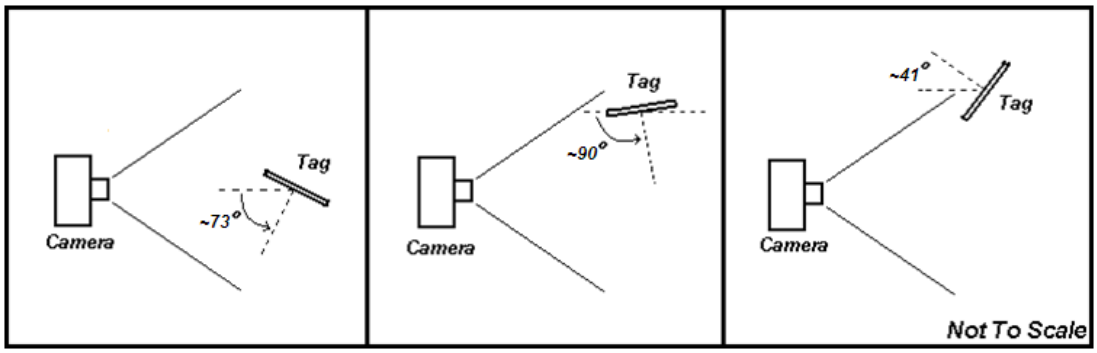

FIGURE 37: TAG-DETECTION ANGLE GRAPHIC

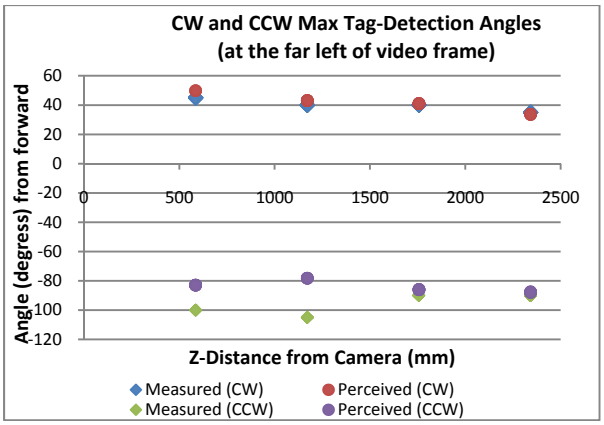

FIGURE 39: TAG-DETECTION ANGLES (FAR LEFT)

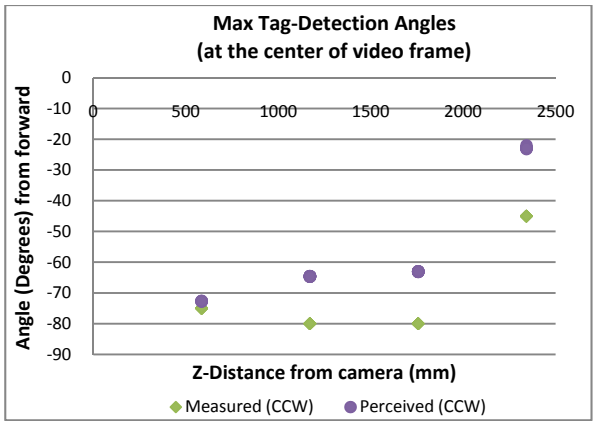

FIGURE 38: TAG-DETECTION ANGLES (CENTER)

Based on the graphs, we determined that the detection angle extremes are dependent on the location of the tag in the video frame. In the graph shown in Figure 39: Tag-Detection Angles (Far Left), on the far-left of the frame, the tag could be detected at about half the range when rotated clockwise from forward as compared to when rotated counter-clockwise from the front. Also, for the graph in Figure 38: Tag-Detection Angles (Center), the maximum rotation angle appeared consistent with the results from the previous graph. If one were to take the range of the detection angles from Figure 39: Tag-Detection Angles (Far Left), the maximum angle in Figure 38: Tag-Detection Angles (Center) falls about at the halfway point in that range. This comparison demonstrated the proportional nature between the position in the frame and the clockwise and counter-clockwise maximum detection angles.

The tables below show the average values for the clockwise and counter-clockwise detection angles for the tag, in both the far-left and center tag test. Both tables show that across the different distances, the standard deviations in the both the measured and perceived angles were somewhat high. Additionally, the difference between the average perceived angle and the measured sometimes differed by nearly 15 degrees in the tests. Despite these non-trivial errors, one can still approximate the detection ranges.

Table 12, the difference between the measured and perceived values was about 13 degrees for the counter-clockwise direction. Taking the average of the perceived and measured values, we can estimate that the maximum counter-clockwise detection angle was about 90 degrees. Conversely, the difference for the clock-wise rotation was much smaller, with an average clockwise detection angle of about 41 degrees. This means that the overall range of detection angles when the tag was located at the far-left of the frame was 131 degrees.

TABLE 12: TAG-DETECTION ANGLES (FAR LEFT)

2 – 8 Foot Range		Average	Std. Dev.
CCW Rotation (degrees)	***Measured***	96.40	6.58
	Perceived	83.62	3.63
CW Rotation (degrees)	***Measured***	40.00	3.49
	Perceived	41.90	5.70

Similarly to the far-left tag test, the data in the center-tag test in Table 13 below had a rather large difference between the measured and perceived angles. Based on the two distance ranges in the table, we determined that the 2-8 foot range has a much larger standard deviation in values than the 2-6 foot range. This is representative of the shape of the graph, where at 8 feet, the detection range seemed to drop off significantly and no longer accurately represented the detection angles in the short-range. Therefore, the 2-6 foot range would probably be more representative of the range of consistent detection angles. Using this subset of the data, we determined the range of maximum detection in both directions is about 73 degrees. This means that the system would be able to detect a 146 degree range of angles.

TABLE 13: TAG-DETECTION ANGLES (CENTER)

2 - 8 ft Range	Average	Std. Dev.		*2 - 6 ft Range*	Average	Std. Dev.
Measured	70.80	14.30		**Measured**	78.38	2.37
Perceived	56.75	18.99		**Perceived**	66.74	4.26

4.2.4 MESSAGE UPDATE RATE

The next step in our analysis of ARToolKit was to determine the maximum message rate of the library to determine how continuously the data was posted for use in the rest of the system. Based on the number of messages being collected per second (sample rate) on the test machine, we created a histogram shown in Figure 40: Histogram of Message Update Rate that demonstrates the rate achieved. This shows that in our particular configuration, about 22-24 messages were sent per second, though this rate is dependent on the hardware employed in the test machine (Intel Core 2 Duo 2.2GHz) and that machine's current CPU load.

We also noticed during testing that if the resolution of the camera was reduced, the message rate would increase, potentially providing a higher frame-rate of capture (relevant to webcams, mostly) and requiring less time to process the data. We observed qualitatively, that the lower resolutions produced an increased number of messages per second.

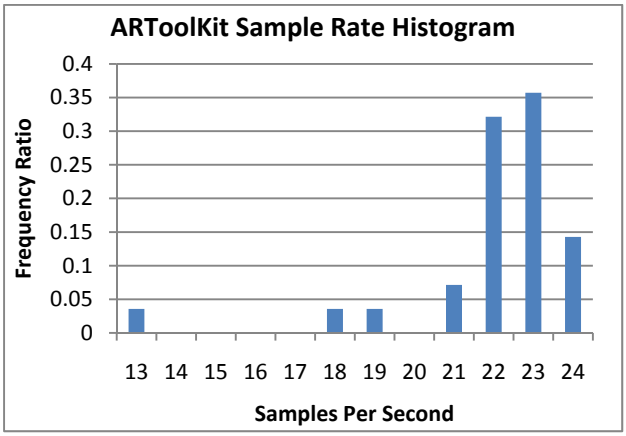

FIGURE 40: HISTOGRAM OF MESSAGE UPDATE RATE

4.2.5 LIGHTING AND TAG OCCLUSION OBSERVATIONS

One of the biggest challenges when performing the tests of ARToolKit was overcoming glare from the lights in the testing area. Because the tag was printed using a laser printer, the black surface was slightly reflective, causing a loss of tag detection when tilted towards the lights, as shown in Figure 41: Effects of Glare on Detection below.

This glare problem illustrated a much larger problem with the ARToolKit library: it does not handle lighting gradients well. This problem was very apparent with shadows as well; the detection ability would severely degrade when shadows were cast on the tag. Additionally, if there was a high contrast between lighting and the shadows cast on the tag, the system would fail to detect the tag. These problems were likely because ARToolKit performs a simple threshold algorithm on the input video stream instead of taking steps to compensate for gradient lighting.

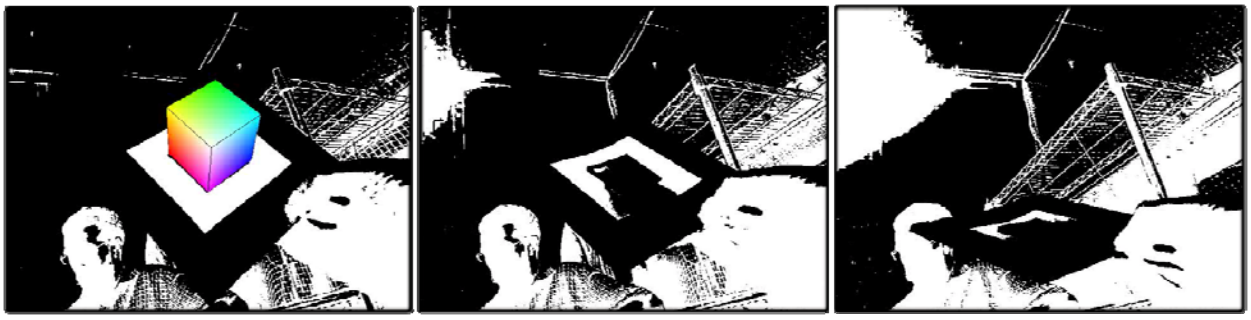

FIGURE 41: EFFECTS OF GLARE ON DETECTION

Next, this system lost detection when the tag was obscured in any way, even if the obstruction was minimal. As shown in Figure 42: Tag-Occlusion Example below, when the tag is obscured even slightly, here by a portion of the thumb, the detection would totally cease. This would be a problem in any real-world situation in which an object could block a portion of the tag periodically. We believed that there is a "confidence" parameter that could be adjusted in the ARToolKit library configuration that could help to lessen this issue.

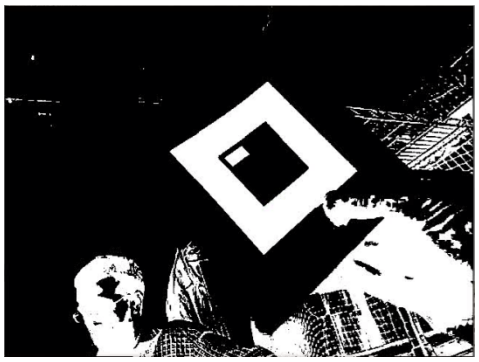

FIGURE 42: TAG-OCCLUSION EXAMPLE

5.0 CONCLUSIONS AND RECOMMENDATIONS

The goals of this project were to develop a PC control interface for the CyberQuad system, enable precise UAV localization, and provide documentation to enable the continued development of the CyberQuad system at MIT Lincoln Laboratory. Over the course of the project, we were able to achieve all of our outlined goals to the level representative of a proof-of-concept design and implementation. The resulting baseline system suggests that highly autonomous quadrotors could be feasible in the near future, utilizing low-footprint vision-based localization systems to aid in take-off and landing procedures.

However, there is still a significant amount of system development which must first occur before an autonomous, vision-guided quadrotor can be fully realized. Specifically to our CyberQuad system, latency problems with the control scheme must first be resolved, followed by significant work in making the localization system more robust. Our observations about the project status and suggestions for future work are outlined below.

UAV LOCALIZATION SYSTEM

With our limited stay on the MIT Lincoln Laboratory campus, we were only able to test ARToolKit with a stationary camera and tag. However, in real-world settings, the ability to consistently track moving (dynamic) tags will be equally as significant as its ability to accurately determine the location and orientation of a fixed target.

To fully quantity the abilities of ARToolKit, or any augmented reality library, we recommend a regimen of testing using the Vicon motion-capture system as a base line. Using this, a tag could be moved around freely in an environment while both the ARToolKit ROS node and the Vicon system gathered position and orientation data. By analyzing the collected data, it would be possible to accurately calibrate and determine the tracking limitations of the system, both with static and dynamic tags. One could more-accurately determine the maximum detection ranges as well as the amount of error one would expect from the system. Additionally,

one could generalize the average position-update rate of the *uav_artag* node in varying environmental conditions and fast-motion scenarios, and also to measure the percent of the time our system fails to, or incorrectly recognizes the target tag.

Generally, we feel further research should focus on multiple tag systems and alternative techniques to expand the limited abilities of the tracking system. We feel that the following plan for development should be observed:

1) First, one must establish a consistent, somewhat robust single-camera tracking system on the UAV. A robust system should be able to track multiple tags (as compared to a single tag per-camera in our system) of multiple sizes, to allow for both close and longer-range detection, as well as provide a failsafe if environmental factors prevent detection of some of the tags. This could also include an investigation into a nested tag system, where smaller tags are embedded within the pattern of a larger tag, allowing for both long and short-range tracking using one condensed tag area.
2) Next, a flexible sensor-fusion system should be developed, enabling multiple cameras to be used both on the UAV and on the ground-station. This system would likely start with adding additional cameras to the UAV, simply providing more data-points from which to make conclusions about the UAV's location and orientation. Next, a feasibility study should be done to see if the same augmented-reality tag system could be used to track the UAV from the ground. If this is not possible, a natural-feature-tracking system could be developed, allowing the ground-station to detect the UAV simply by its silhouette against the sky, providing a failsafe if one of the two vision systems is shut down completely.

UAV CONTROL SYSTEM

With our current system, problems with system performance would prevent any real-time closed-loop UAV control in the future, unless changes are made. The system communicated

with the CyberQuad device and could send commands, but the system was far from usable, having problems both with the ROS system and apparently with the serial link.

Because there were visible reductions to the control-computer's performance when running the full stack (all of the CyberQuad associated nodes, localization and control loops), the low-latency, fast-response-time system required for UAV control was simply not present. Future work with this system should seek to mitigate these performance problems by seeking to streamline the software, as well as by running the ROS nodes in a distributed manner (running resource intensive nodes, *uav_artag* and *uav_adapter*, on separate machines). This functionality is already supported by the ROS architecture, so minimal effort will be required to eliminate one of the potentially highest causes of system latency.

Additionally, our system exhibited noticeable lag between receiving input (via the joystick or other control node), packing and sending commands, and the CyberQuad's physical response to these commands. Though these problems could have been a result of the poor performance of the hardware running the ROS nodes, another possibility is that the serial connection itself was actually over-loaded, with too much data being passed over the low-data-rate connection. Alternatively, the ZigBee wireless serial connection was simply dropping too many packets.

The delayed response may also have been the result of limitations present in the CyberQuad's *MikroKopter* hardware. In our configuration, control messages sent to the quadrotor are first processed by the *NaviCtrl* board, and then forwarded to the *Flight-Ctrl* board before being executed. This introduces a small, but finite latency not experienced by commands sent by the analog controller.

Therefore, research should be conducted to analyze the serial connection and determine if messages are being dropped or delayed, and where the problem is occurring in the message pipeline.

Overall, if this lag problem cannot be resolved, alternative methods of system interfacing must be investigated. A computer-controlled analog control emulator (effectively a radio-control dongle) would allow for more continuous computer communication to the quadrotor, replicating the exact communication scheme employed by the current analog controller. If this suggestion did not mitigate the problem, work would likely need to be done to offload all localization processing and control onto the CyberQuad itself, significantly reducing the data-rate requirements for the serial connection.

FUTURE CONTROL SYSTEMS

There is still significant software development required before the CyberQuad can be used in real world collaborative robotic projects. Our project focused on the goal of obtaining basic computer control over the UAV. While we accomplished this, before any ground-air coordination can occur, conceptually higher levels of control of the UAV must be created to automate landing, takeoff, and mission execution procedures. This would require developing complex control algorithms and procedures, far out of the scope of this project.

To aid in this development, we recommend using the Vicon system for the free-flight testing of the UAV. By collecting data on the orientation of the UAV in flight with the Vicon system, it would be possible to generate a better dynamic model for any control scheme eventually implemented in software. Likewise, the Vicon system would be a good means to measure the performance of the current feedback control code or, in our case, the augmented-reality tag-tracking system. We recommend sensor-fusion integration between the vision system and onboard IGS systems required achieve a truly robust system in future project iterations.

Eventually, we foresee extensive work being done in the areas of waypoint programming for mission planning, with long range trajectory coordination between the UAV and ground-based system. At this point, the take-off and landing procedures, as well as several others, would be fully automatic, fully accomplishing the vision of MIT Lincoln Laboratory and this project overall.

RESOURCE OBSERVATIONS

With regards to the localization system, we would recommend investigating augmented reality libraries other than ARToolKit. ARToolKit was readily available during the period of our project, but research shows that a number of superior and more up-to-date alternatives exist. With the framework we have established, it should be relatively easy to replace with a commercial product that is available or will be available in the near future. It simply did not prove usable under the conditions which would make this feasible in outdoor, real-world environments.

Additionally, with regards to the UAV system chosen for MIT Lincoln Laboratory, we would tentatively recommend future quadrotor work be developed on systems not sold by Cyber Technology, or at least not this specific system. Throughout our project we had a number of issues that can be attributed, at least in part, to this company's lack of experience and quality control of CyberQuad product. The quality of the provided quadrotor and product support simply did not reflect its price. Moreover, the prohibitive cost of the quadrotor in many cases limited our ability to experiment, as we were significantly more cautious than we might have been with a similar, less-expensive system.

WORKS CITED

[1] United States Department of Defense. (2003, June) Department of Defense. [Online]. http://www.defense.gov/specials/uav2002/

[2] United States Air Force. (2010, July) Fact Sheet: MQ-1 PREDATOR. [Online]. http://www.af.mil/information/factsheets/factsheet.asp?fsID=122

[3] Radu Horaud, Bernard Coni, and Oliver Leboulleux, "An Analytical Solution for the Perspective-n-Point Problem," *Computer Vision, Graphics, and Image Processing*, pp. 33-44, 1989.

[4] Jacob Sauer. (2007, October) Lincoln Laboratory Intranet: Education Program Course Listing Archive. [Online]. http://llwww.llan.ll.mit.edu/Education/LEP/Archive/0607/TechAware/Lecture3/06-Sauer.pdf

[5] Cyber Technologies. (2010) CyberQuad Overview. [Online]. http://www.cybertechuav.com.au/-Overview,85-.html

[6] MikroKopter. (2010, August) MikroKopter Wiki. [Online]. http://www.mikrokopter.de/

[7] MikroKopter. (2010, August) QMKGroundstation. [Online]. http://www.mikrokopter.de/ucwiki/QMKGroundStation

[8] Willow Garage. (2010) ROS. [Online]. http://www.ros.org/wiki

[9] Cesar Vargas, *Position Location Techniques and Applications*. New York: Elsevier, 2009.

[10] A Masselli, S Scherer, and K Wenzel. (2010, May) Autonomous Flying Robots. [Online]. http://www.ra.cs.uni-tuebingen.de/forschung/flyingRobots/welcome_e.html

[11] S Lange, P Protzel, and N Sunderhauf, "A vision based onboard approach for landing and position control of an autonomous multirotor UAV in GPS-denied environments," *Advanced Robotics*, pp. 1-6, 22-26, 2009.

[12] P Rosset, K Wenzel, and A Zell, "Low-Cost visual tracking of a landing place and hovering flight control with a microcontroller," *Journal of Intelligent & Robotic Systems*, pp. 297-311, 2009.

[13] M. Achtelik, K. Kuhnlenz, Tianguang Zhang, and Ye Kang, "Autonomous hovering of a vision/IMU guided quadrotor," *Mechatronics and Automation*, pp. 2870-2875, 9-12, 2009.

[14] (2007) An Introduction to ARToolkit. [Online]. http://www.hitl.washington.edu/artoolkit/documentation/userintro.htm

[15] Aerospace Industries Ltd. (2002) Heron 1. [Online]. http://www.iai.co.il/18900-16382-en/BusinessAreas_UnmannedAirSystems_HeronFamily.aspx

[16] George Schmidt and Richard Phillips. (2004) NATO, RTO. [Online]. http://ftp.rta.nato.int/public//PubFullText/RTO/EN/RTO-EN-SET-116///EN-SET-116-04.pdf